L-vehicles Emissions and Noise mitigation Solutions

D5.2 Techniques for tampered/high-emitting LV detection

This project has received funding from the European Union's Horizon Europe research and innovation programme under grant agreement No 101056777

Deliverable No.	5.2	
Deliverable title	Techniques for tampered/high-emitting LV detection	
Deliverable type	Report	
Dissemination level	PU - Public	
Deliverable leader	KU Leuven	
Contractual due date	31.08.2024	
Actual submission date	31.08.2024	
Version	1.0	
Written by	Hervé Denayer, Hongxun Gu, Konstantinos Gryllias (KU Leuven), Martin Kupper (TU Graz)	07.08.2024
Reviewed by	Frank Schwarz (BMW) Leon Ntziachristos (EMISIA)	21.08.2024
Approved by	All partners	30.08.2024

Disclaimer

Funded by the European Union. Views and opinions expressed are however those of the author(s) only and do not necessarily reflect those of the European Commission or CINEA. Neither the European Commission nor CINEA can be held responsible for them.

Revisions table

Version	Date	Change
1.0	31.08.2024	First submission to the EC

This project has received funding from the European Union's Horizon Europe research and innovation programme under grant agreement No 101056777

Table of contents

This project has received funding from the European Union's Horizon Europe research and innovation programme under grant agreement No 101056777

Executive summary

This deliverable of the LENS project focuses on the development of the techniques for detecting tampered/high-emitting L-category vehicles based on roadside measurements of noise and pollutant emissions. The approaches based on noise and pollutants have first been developed as independent systems and their measurement results will be synchronized in postprocessing. For noise, a measurement setup has been defined for the LENS in-field surveys, signal processing routines have been implemented and a preliminary analysis of promising features for tampering detection has been carried out using available datasets. These techniques will be developed into a tampering detection method based on the noise measurements to be collected during the in-field surveys. For pollutants, devices for point sampling have been benchmarked against reference instruments and the results show very good correlation for all measurements. Additionally, an optical Schlieren imaging system to visualize the spread of the plume has been developed and tested. In preparation of the in-field surveys later in the LENS project, all noise and pollutant measurement systems have been deployed together and thoroughly tested during a validation measurement campaign at TU Graz.

List of abbreviations

AI	Artificial Intelligence
ANPR	Automatic Number Plate Recognition
BC	Black Carbon
BOS	Background Oriented Schlieren Imaging
CFR	Cylinder Firing Rate
CNN	Convolutional Neural Network
CS	Catalytic Stripper
CSM	Cross-Spectral Matrix
EC	Elemental Carbon
EEPS	Engine Exhaust Particle Sizer
EFR	Engine Firing Rate
L-vehs	L-category vehicles
MFCC	Mel-Frequency Cepstral Coefficients
OC	Organic Carbon
PR	Prominence Ratio
PS	Point Sampling
PSF	Point Spread Function
RDC	Real Driving Cycle

This project has received funding from the European Union's Horizon Europe research and innovation programme under grant agreement No 101056777

RPM	Revolutions Per Minute
SK	Spectral Kurtosis
STFT	Short-Time Fourier Transform
TFR	Time-Frequency Representation
TTNR	Tone-To-Noise Ratio
WP	Work Package
WT	Work Task

List of figures

This project has received funding from the European Union's Horizon Europe research and innovation programme under grant agreement No 101056777

List of tables

This project has received funding from the European Union's Horizon Europe research and innovation programme under grant agreement No 101056777

1 Introduction

1.1 Background and objectives

Noise and air pollution due to road traffic are widely recognised as two of the most important threats to human health and wellbeing. L-category vehicles are an important contributor to both types of pollution due to the less strict emission standards compared to passenger cars and because the noise character of certain types of L-vehicles is also often perceived as particularly annoying. Especially tampered vehicles, which have been modified to alter the performance or to modify the sound of the vehicle, are important contributors to the pollutant and noise emissions [1], and hence the annoyance and health impacts caused by them.

This report is the deliverable of Task 5.2 of the L-vehicles Emissions and Noise mitigations Solutions (LENS) project, which focuses on roadside detection techniques for tampered and high-emitting L-category vehicles. The goal of this task is to develop and validate the measurement setups and detection algorithms which will be used for the in-field surveys in Task 5.3. In particular, the main objectives of this task are:

- Designing the system specifications and the implementation blueprints.
- Acquiring microphones and arranging their position in relation to emission measurement devices.
- Acquiring the emission measurement devices and cameras for license plate recognition.
- Integrating a PN sensor in the remote emission sensing system.
- Validating the integrated system on a test-track before executing the main field surveys in WT 5.3.

1.2 Approach and outline

The tampering detection approaches based on noise and pollutant emissions respectively have first been developed as independent systems. The development of the method based on noise measurements is detailed in section 2, the approaches focusing on pollutant emissions using point sampling and Schlieren imaging systems are detailed in, respectively, sections 3 and 4. During a validation campaign, all systems have been synchronized and tested on a variety of motorcycles. This measurement campaign and its main results are discussed in section 5. The main outcomes of this deliverable are summarized in the concluding section 6.

This project has received funding from the European Union's Horizon Europe research and innovation programme under grant agreement No 101056777

2 System for tampering detection using noise measurements

2.1 Literature review

Equipment for monitoring environmental noise levels has been commercially available for decades. However, such systems only provide overall exposure levels, for example, the equivalent sound pressure level L_{eq} or the day-evening-night level L_{DEN}, and no information on the contributions of individual vehicles. Although a single loud vehicle passing by typically doesn't have a major impact on these exposure levels measured over a longer duration, such short but loud events are often the basis for noise complaints. Over the last decade, research organisations and commercial players therefore started developing dedicated roadside measurement systems for individual sources of traffic noise. Most systems combine a microphone array with other sensors, such as cameras, to monitor the noise levels of individual vehicles and/or to identify too loud vehicles.

The French non-profit environmental organisation Bruitparif has developed the patented 'Medusa' measurement system to determine the sound level and origin of dominant noise sources [2]. It consists of four microphones to localise sound sources and projects the results on images taken with a wide-angle fisheye camera. This system has been further developed into the 'Hydra' noise camera, which enables the enforcement of noise limits on individual vehicles [3]. The system combines two medusa subsystems with two ANPR cameras and one wide-angle fisheye camera. The system cross-references the data collected with the two four-microphone arrays of the Medusa units and, if the noise levels exceed the legal limit, compares the trajectory of the detected dominant noise source with the trajectory of the vehicles automatically extracted from the camera images.

The MicrodB group based in Lyon has developed the dBFlash system, which is also capable of detecting and enforcing against excessively noisy road vehicles [4]. The system uses a linear microphone array, combined with cameras for linking the noise measurements to individual vehicles and for automatic number plate recognition. The detection procedure includes noise level qualification, estimation of the vehicle speed and automatic vehicle identification.

The Noisy vehicle surveillance camera (NoivelCam) system developed at Nanyang Technological University has a similar goal as the Hydra and dBFlash systems, but uses 2 highly directive microphones installed above the road instead of a microphone array installed at the roadside [5]. The system focuses on a single lane and triggers a high-speed camera to register the license plate of vehicles exceeding the noise limits.

Within the recently completed H2020 NEMO project [6], an autonomous system was developed to measure an individual road or rail vehicle's noise emissions in a traffic stream. The system uses a microphone array, combined with a doppler radar and an ANPR camera, to locate and quantify noise sources and determine whether these vehicles are high emitters or not. The system is also capable of detecting the origin of the noise for an individual vehicle, separating contributions from the engine and the tire-road interaction.

Noise measurement systems like the ones discussed above have been tested in the field at various locations and several countries are considering the use of such systems for enforcing noise limits [7]. However, these

This project has received funding from the European Union's Horizon Europe research and innovation programme under grant agreement No 101056777

systems and pilot projects focus on identifying excessively loud vehicles, irrespective of this is due to the state of the vehicle itself (tampering, poor maintenance, …) or the driving behaviour (high engine RPM in low gear, high acceleration, …). LENS instead focuses on the identification of tampered L-category vehicles based on their sound measured from the roadside. Since the measurement distance, the road conditions and many other factors influence the measured sound pressure levels, a method based on characteristics (signal features) of the vehicle sound rather than absolute noise levels is expected to be more reliable [8][9][10]. The development of techniques to automatically detect anomalies or classify events based on characteristics of sound signals is a very active research domain and techniques have already been presented for a wide range of applications, such as detecting incidents in road tunnels [11], detecting defects in bearings of passing rail vehicles [12][13], classifying sound events such as passing vehicles into different categories [14][15], and much more. These approaches aim to detect certain characteristics of the sound signals and use these features to perform the anomaly detection or classification.

Recently, researchers also started investigating such approaches to detect vehicles with modified exhaust systems. The Japanese National Traffic Safety and Environment Laboratory is working on an automated roadside system to detect illegal aftermarket silencers, as alternative for labour-intensive stationary noise tests [8][9]. Their method uses a microphone array to measure the sound of passing vehicles and to separate the contribution of an individual vehicle and uses an AI model to classify the vehicle as legal or illegal. The classification model is based on time-frequency diagrams stored as images and was trained using a dedicated dataset, collected using 3 L3 category vehicles with a legal muffler and 3 with an illegal aftermarket silencer at various speeds and accelerations. Cheng et al. recently presented an approach to detect passenger cars with modified exhaust systems [10]. They collected a large dataset of recordings of passing vehicles under real-life driving conditions and trained a Convolutional Neural Network (CNN) to classify the vehicles according to the suspected state of their exhaust system (modified or unmodified). Similar to the previous approach, this method is based on spectrograms of the recordings stored as images. Within LENS, the goal is to develop a technique to detect tampered L-category vehicles based on the characteristics of their sound, possibly combined with their emission levels, both measured from the roadside. The following sections discuss the different elements of the toolchain developed for this purpose.

2.2 Measurement setup

The goal of the LENS project is not to develop a new hardware system for roadside noise measurements as it is clear from the literature review that different suitable systems are already on the market. Instead, the focus is on the development of signal processing techniques and a measurement setup has been assembled for executing the LENS in-field surveys using commercially available microphones and acquisition systems. This approach provides full control over the acquisition settings and unrestricted access to the raw measurement data.

The noise measurement setup consists of a linear array of 5 microphones, connected to a data acquisition system and controlled via a laptop, on which the data is stored locally. Batteries provide the necessary electric power to operate the complete system. The Siemens Scadas XS acquisition system [16] is controlled via its “Simcenter Test.Lab” software and dedicated scripting automating the measurement process. The system is programmed to continuously monitor the A-weighted sound pressure level (LAF) at the first microphone of the array and to start recording the signals from all microphones when a threshold is exceeded. Based on the outcome of the validation measurement campaign (see section 5.2.1), this

This project has received funding from the European Union's Horizon Europe research and innovation programme under grant agreement No 101056777

threshold is set on-site and continuously reevaluated during the measurement campaign as it highly depends on the local situation (background noise, distance between the microphones and the driving lane, etc.). Each recording lasts for a minimum duration, which is also set on-site depending on the traffic intensity and spacing between vehicles, and stops after this duration when the sound pressure level at the first microphone position drops below a threshold. This threshold is usually set equal to the threshold for starting a recording, but can be adapted independently if needed. Even though it is expected that the information on the vehicle state is mostly contained in the low frequency noise, the sampling frequency of the system has been set to 25600 Hz.

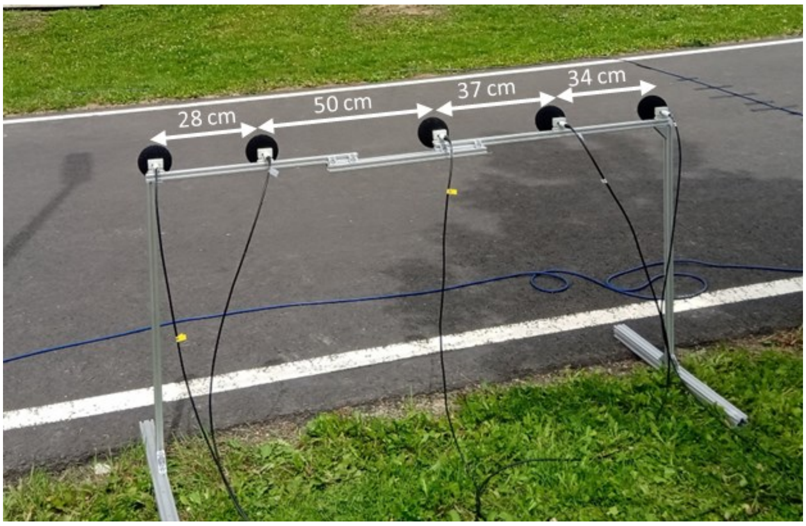

Figure 1: Configuration of the microphone array.

Water- and dust resistant ½" array microphones (type PCB 130A24 [17]) with wind screens have been selected for the microphone array. These microphones offer a good compromise between the consistency of their frequency and phase response needed for multichannel applications, and cost. Although a 2D array with many microphones capable of pinpointing the exact location of a source could be used, detecting the driving direction of the passing vehicles should be sufficient for traffic conditions expected during the LENS measurement campaigns. A more cost-effective linear array topology with 5 microphones, which can only identify the angle of arrival of the sound with respect to the roadside, is therefore selected. The array design has been obtained by optimizing the point spread function (PSF), representing the capacity of the array to focus on a point source at a specific angle. Based on the preliminary testing carried out with different array configurations, this optimization has been performed considering a harmonic point source at 40 Hz located in front of the array and imposing a limit of 1,5 m on the total array length for practical reasons. The optimized microphone array, shown in Figure 1, yields an open angle of 66 degrees for a reduction of 3 dB as shown in Figure 2. In comparison, an equidistant microphone array of the same length gives an almost flat PSF and a reduction of less than 0.05 dB at both ends. With the optimized array and the corresponding signal processing techniques, it is possible to trace the relative position of the moving vehicle in terms of the angle with respect to the axis perpendicular to the array and as a function of time. This allows identifying the driving direction of a vehicle from the noise measurements. Additionally, also a rough estimation of the vehicle speed could be obtained. More details on the array signal processing technique are provided in section 2.3.1.1. The height of the microphones is not expected to have a major impact on the measured

This project has received funding from the European Union's Horizon Europe research and innovation programme under grant agreement No 101056777

noise signatures and has been set to 1,2 m, similar to the test setup for pass by noise measurements described in the ISO 362 standard.

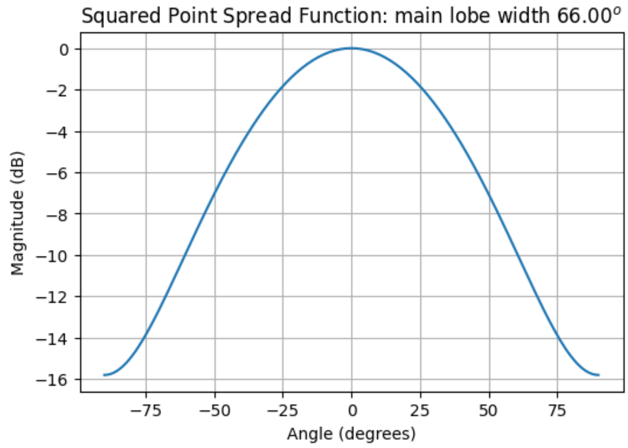

Figure 2: Point Spread Function (PSF) of the optimized microphone array.

2.3 Signal processing

The tampering detection algorithm is envisaged as a modular toolchain, using the measured time signals as input and applying a series of signal processing techniques. The main building blocks of the toolchain are:

1) the number of preprocessing steps, including a source localization algorithm to separate contributions of different vehicles, the computation of spectrograms and the identification of the engine orders in the spectrum;
2) the computation of a range of features, which can be an indicator for the state of the vehicle, from the preprocessed signals; and
3) the anomaly detection algorithm, which uses a set of features as input.

The following sections of this deliverable detail the different building blocks which have been implemented, in preparation of the in-field surveys. The actual detection algorithm will be developed using the data captured during these measurement campaigns. Its implementation and performance will be discussed in detail in D5.3 of the LENS project.

2.3.1 Preprocessing

2.3.1.1 Source localisation

Since noise propagates over large distances, it is not possible to assume that only vehicles driving on the nearest lane, which are the focus of the investigation, will trigger the start of a measurement. Also, it is possible that a recording contains contributions of 2 or more vehicles following each other closely. As discussed in the introduction, approaches are available to separate – within certain limits – the contribution of an individual vehicle in a traffic flow and it is not the goal of LENS to develop a new method for vehicle noise source identification. Nevertheless, the signals recorded during the LENS measurement campaigns will need to be attributed to a vehicle and identifying the lane on which it is driving, and hence the driving direction, is crucial to ensure a consistent dataset. It may also be needed to split signals according to the

This project has received funding from the European Union's Horizon Europe research and innovation programme under grant agreement No 101056777

dominant contributor before further processing. A simple source localization algorithm has therefore been implemented as the first building block of the signal processing toolchain.

The beamforming technique CLEAN-PSF [18] is applied to track the dominant energy trajectory (angle) of a moving source with respect to the centreline of the array and as a function of time. The technique considers one angle of incidence at a time and computes a weighting vector defined by steering vector for that angle, which depends on the array configuration. The energy for that specific direction is then obtained by calculating the norm of the projection of measured cross-spectral matrix (CSM) on the weighting vector. The algorithm then subtracts the contribution of the dominant steering vector (direction) from the measured CSM and repeats this procedure for the next dominant vectors until no dominant vector can be extracted from the residue of the measured CSM. The final beamforming map is then the summation of the first N extracted dominant vectors.

2.3.1.2 Time-frequency representation of the measured signals

Time-frequency representation (TFR) plays a crucial role in many anomalous sound-event detection techniques. It allows analysing non-stationary signals by illustrating how the frequency components of the signal change over time. Such patterns are often excellent candidate features for anomaly detection or sound classification, as illustrated by the many studies, including the ones on illegal replacement muffler detection [8][9][10], using such representation of the measured signals. TFRs are usually obtained using a short-time Fourier transform (STFT) and are represented on linear, logarithmic or mel-scales depending on the application, but alternatives such as the wavelet transform could also be used. For the results presented in this deliverable, the STFT is used and the settings are carefully chosen for each dataset as a trade-off between the time resolution, i.e. the ability to track transients, and frequency resolution, i.e. the possibility to identify tones such as the engine orders (see section 2.3.1.3).

2.3.1.3 Extraction of engine orders

Combustion engine noise is characterised by strong tonal components, so called orders, related to the rotational speed of the engine. The dominant frequency components for engines with evenly spaced firing intervals are the cylinder firing rate (CFR) and engine firing rate (EFR), which are related to the engine RPM as follows:

$$\mathrm{CFR} = \frac{\mathrm{RPM}}{60}\frac{S}{2}\ [\mathrm{Hz}] \qquad\qquad \mathrm{EFR} = N\,\mathrm{CFR}$$

With $S = 1$ for 4-stroke engines and $S = 2$ for 2-stroke engines and N the number of cylinders of the engine. Also higher harmonics of these frequency components can be clearly distinguished. The noise spectrum of engines with uneven firing intervals will also exhibit distinct frequency components related to the engine RPM and the firing order determines which of them are the most prominent. These frequency components, so-called engine orders, play a pivotal role in the human perception of the vehicle sound and vehicle modifications aiming to modify the sound character will almost certainly affect the energy distribution over the different engine orders. Identifying these orders in the measured spectra can therefore be a key enabler for tampering detection.

For roadside measurements, the frequencies need to be corrected for the Doppler effect. This can be done by resampling the signals if the vehicle speed is known. However, since this correction is negligible for low vehicle speeds as will be the case in the LENS in-field surveys and given the fact that the goal is not to

This project has received funding from the European Union's Horizon Europe research and innovation programme under grant agreement No 101056777

extract the exact engine RPM from the measurements, it is decided not to apply any correction for the Doppler effect.

Several techniques could be applied to identify engine orders in the time-frequency diagram of the measured signals. Although more efficient and elegant algorithms exist to estimate the fundamental frequency in a spectrum using for example cepstrum analysis [19], an approach based on a sliding comb filter has shown to be more robust for a wide range of vehicles and conditions. The algorithm loops over a relevant range of fundamental frequencies, determined based on the typical RPM range and the type of engine. For each fundamental frequency, a filter $H(f)$ is defined which extracts the this frequency and its multiples from the spectrum:

$$H(f) = \left[(1+\alpha^2) - 2\alpha\cos\left(2\pi(f/f_0)\right)\right]^{-1/2}$$

The parameter α controls the width of the peaks of the filter and needs to be set in correspondence with the frequency resolution of the spectrum used as input. The filter is then applied to each line of the spectrogram. For each time instance, the filtered spectrum is integrated up to a predefined order and scaled with the corresponding bandwidth. The fundamental frequency yielding the highest value for the filtered and integrated spectrum is identified as the dominant family of engine orders at that time instance. This should be the 1st or 1/2th engine order for, respectively, 2-stroke and 4-stroke engines with even firing intervals. For engines with uneven firing intervals, it can be the order corresponding to the periodicity of the full cycle.

2.3.2 Feature selection and engineering

With the limited datasets currently available, only features selected based on literature and physical insights have been studied. These features will then be processed for the anomaly detection method once labelled measurement data for both tampered and untampered L-category vehicles become available from the field measurements with roadside inspections. Based on these results, the current set of features could still be extended with additional or improved engineered features. Additional features can then also be extracted via AI methods applied directly to raw or pre-processed time signals. The following sections provide an overview and short description of the current selection of signal features.

2.3.2.1 Time domain features

Time domain features are computed directly from the measured signals without prior preprocessing and are therefore often used in applications where computational efficiency is of the essence and near real-time decisions need to be made. Common features used for anomaly detection or classification include rolling statistics, obtained by computing statistical quantities of the signals over a sliding window. The mean of a sound pressure signal should be zero by definition and is not a useful feature for the detection of tampered L-category vehicles. Also measures for the signal magnitude, such as the mean absolute value or the root mean square, will not be considered as the signal amplitude is directly related to the sound pressure level which depends on many other variables than the state of the vehicle [10]. For the same arguments, also the standard deviation and variance are not considered as possible features. Instead, normalised high order statistical features could contain valuable information for tampering detection:

- **Skewness** is a measure for the symmetry of the distribution compared to a normal distribution.
- **(Excess) kurtosis** is a measure for the importance of the tail of the distribution. It is often used as a metric for the impulsive character of the signal.

This project has received funding from the European Union's Horizon Europe research and innovation programme under grant agreement No 101056777

2.3.2.2 Frequency and time-frequency domain features

The spectrogram can be used directly as input for an AI model, as was done in different studies aiming to detect modified exhausts using roadside measurements [8][9][10] and will be studied within LENS once suitable data is available from the in-field surveys. However, it is also possible to first compute additional features from the TFR to extract specific information from the signals.

Simple spectral features, such as the relative level between certain frequency bands, can most likely already provide a good indication of tampered exhaust systems. Also the temporal evolution of these metrics during the pass-by event can contain valuable information on the dominant sources of sound and hence the state of a vehicle. Other features which can be computed from e.g. the Mel-Frequency Cepstral Coefficients (MFCC), spectral kurtosis (SK) and the tracked engine orders, which can easily be obtained from the TFR. MFCC are often an excellent feature for sound classification as witnessed by the large number of techniques relying on these features, often in combination with AI methods [20]. SK is a powerful indicator for transient behaviour in the frequency domain, widely used for diagnostics of rotating machinery [21][22]. The orders are directly related to the operation of the combustion engine and radiate from the intake and exhaust system, and hence carry valuable information about the state of these systems.

In summary, the following frequency domain and time-frequency domain features can be studied as indicators for tampered L-vehicles:

- **Spectral content**: e.g. the centre of gravity of the (1/3) octave band spectrum, the difference between the level of the 1/3 octave band or critical band containing the EFR and the overall sound pressure level.
- **The time evolution of the spectral content:** e.g. the duration between the time instances where a relative level drops 6 dB below its maximum value.
- **Engine orders:** the number of engine orders identified in the spectrum before, during and after the passage of the vehicle, the energy content contained in the engine orders compared to the overall sound pressure level.
- Features extracted from **Mel-Frequency Cepstral Coefficients** and their time evolution or **Spectral kurtosis.**

2.3.2.3 Psychoacoustic features

Psychoacoustic metrics aim to quantify certain aspects of the human perception of sound. In the framework of tampering detection, metrics focusing on the tonal content of the spectrum are potentially good indicators for tampering. The reason is that the sound character, which is sometimes the target of the tampering and which is an important aspect of the annoyance caused by L-vehicles, strongly depends on the audibility of specific engine orders. The following psychoacoustic metrics will be investigated as potential indicators for tampering:

- **Tone-To-Noise Ratio (TTNR)**: as illustrated in ***Figure 3***, this metric quantifies the level of tones (= peaks) in the noise spectrum compared to the level of the broadband masking sound. Tones are identified as audible if this relative level exceeds a threshold of 8dB [23]. Several features can be directly obtained from this result, such as the TTNR of the loudest tone, the (maximum) number of prominent tones or the ratio, etc.

This project has received funding from the European Union's Horizon Europe research and innovation programme under grant agreement No 101056777

- **Prominence Ratio (PR)**: this metric is similar to the TTNR, but quantifies the relative level between the critical frequency band containing the tone and the neighbouring (masking) bands as illustrated in Figure 3. By working in critical bands, this metric considers all tones present in a critical band together, whereas TTNR focuses on individual tones [23].
- **Roughness**: is a metric for the modulation of a sound, as occurs due to the series of engine orders characterizing combustion engine sound. Roughness focusing on modulation frequencies which are perceived as a rough sound by the human hearing, i.e. between approximately 20 Hz and 300 Hz. The spacing between the dominant orders for a combustion engine almost certainly falls in this range.

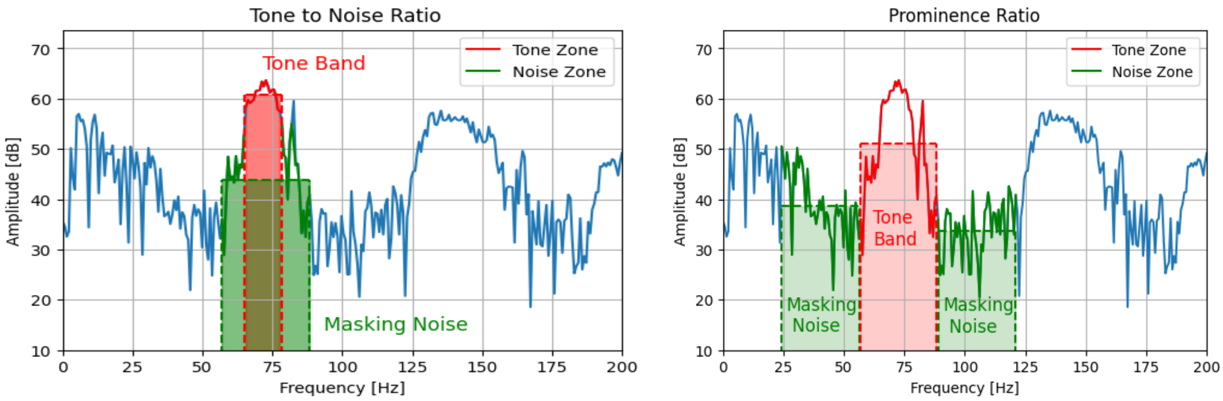

Figure 3: Computation of the tone-to-noise ratio and prominence ratio from a measured spectrum.

It should be noted that the ECMA 418-1 standard [23] describing the TTNR and PR also specifies the measurement environment and how the signal acquisition and processing should be performed. Given the different objectives, this deviates on several aspects from the measurement approach used for the tampering detection. However, a consistent computation of psychoacoustic metrics inspired by the algorithms described in the standards can nevertheless be done to obtain tampering indicators.

2.3.3 Anomaly detection

The actual tampering detection method will process the features computed from the measured signals or extracted via AI methods using semi-supervised learning methods, to avoid labelling of the entire training data set. Models such as Generative Adversarial Network (GAN), Support Vector Machine (SVM) and (Deep) Support Vector Data Description (SVDD) variants will receive special attention since they comprise a particularly active area of research with considerable success for anomaly detection in industrial machinery [24][25].

The training of these algorithms starts from a labelled dataset containing noise signals from tampered and untampered L-category vehicles, measured under comparable conditions. Such dataset will become available from the in-field surveys foreseen in WT 5.3 of the LENS project. The results of these analyses will be reported in D5.3.

This project has received funding from the European Union's Horizon Europe research and innovation programme under grant agreement No 101056777

2.4 Preliminary analysis of features

2.4.1 Noise measurement datasets

In preparation of the in-field surveys, a preliminary analysis of possible tampering indicators has been carried out using available datasets. Besides the noise measurements carried out in the framework of the validation measurement campaign (see section 5.1), several smaller datasets have been used to test the implementation of the signal processing algorithms and to perform an initial selection of tampering indicators. These datasets are:

- **TNO dataset**. TNO kindly provided a dataset with 11 single channel recordings of loud events involving a motorcycle from a measurement campaign in Amsterdam [26]. It is suspected that several motorbikes in this dataset have been tampered with, but no detailed description of the vehicle status is available. The measurements were stored as wav-files, which means the signals are normalized and no absolute levels can be computed.
- **KTM dataset**. KTM kindly provided the recording of a pass by noise test on a Husqvarna Svartpilen 125. As this is a type approval test, the vehicle in mint condition and a detailed description of the test setup is available in the applicable standard. The dataset contains a single run, recorded by 2 microphones: one on either side of the test track.
- **KU Leuven (Diepenbeek) dataset**. Preliminary noise measurements were carried out by KU Leuven in the framework of WT5.2. The dataset consists of several runs past a linear array of 6 microphones with a BMW R1200 motorbike. The dataset contains runs at various speeds and accelerations, but only a rough indication of these quantities is available. The dataset also contains a number of runs with gear shifting in front of the microphone array. The campaign primarily focused on the optimisation of the microphone array and therefore contains measurements using various array layouts. The motorbike use for these measurements is well-maintained and has not been tampered with.

The most important properties of the datasets are summarized in Table 1. Unfortunately, there is no dataset available with labelled recordings of both tampered and untampered vehicles measured with an identical setup. Only a qualitative analysis, based on the comparison between the TNO dataset with measurements on (likely) tampered vehicles and the other datasets with measurements on untampered vehicles, and a preliminary selection of tampering indicators is therefore presented in the following sections.

Table 1: Overview of the noise datasets used for the preliminary analysis of signal features.

	TNO	KTM	KU Leuven (Diepenbeek)	LENS Validation Measurement Campaign
Number of vehicles	11	1	1	5
Number of successful noise recordings	11	1	24	82
Number of microphone channels per recording	1	2	6	5
Microphone array layout	Single channel	1 microphone on each side of the track	Linear array with variable equidistant spacing	Optimised linear array
Vehicle state	Some suspected of tampering	Not tampered	Not tampered	Not tampered

This project has received funding from the European Union's Horizon Europe research and innovation programme under grant agreement No 101056777

2.4.2 Time-segmentation of the recordings

The computed features need to extract characteristics of the passing vehicle and should not be influenced by other vehicles or the background noise. Based on the observations of the validation measurement campaign (see section 5.2.1), only a short time segment of the recording is therefore used to compute the features. This segment, where the vehicle is close is selected based on the A-weighted sound pressure level LAF, which reaches a maximum when the vehicle is closest to the microphone array and dominates the measured noise. The time segment used for further processing is the part of the recording during which the A-weighted sound pressure level remains above a fixed threshold, defined as the maximum value LAFmax during the passing of the vehicle minus 6dB. This approach is illustrated in Figure 4.

The spectrogram of the same signal is shown in Figure 4. This figure illustrates that the pattern of engine orders, which is characteristic of the passing vehicle, is most clear in the selected time segment. This provides confidence that the passing L-category vehicle is the dominant source of sound during the entire duration of the selected time segment of the recording and hence, that the computed features are characterizing this vehicle and not its surroundings.

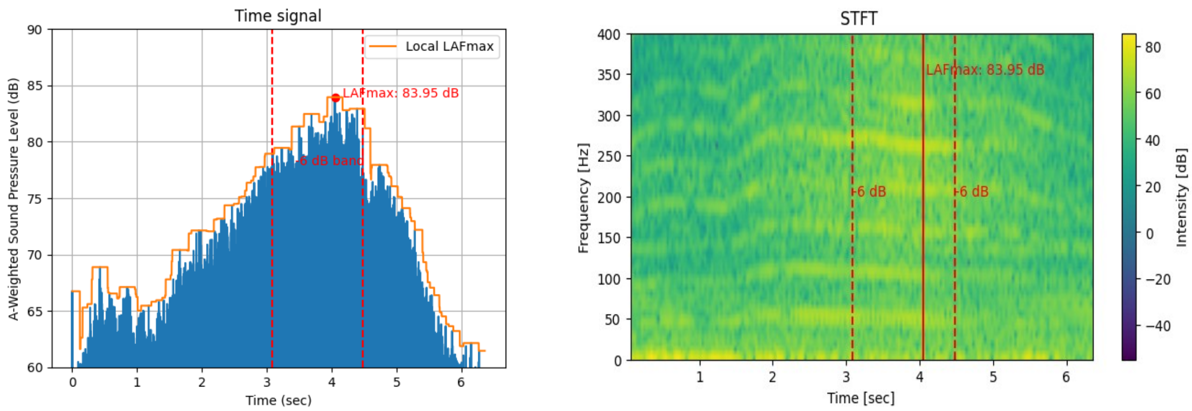

Figure 4: A-weighted sound pressure level as a function of time for a recording of the validation campaign and the corresponding spectrogram, illustrating the time segmentation of the recordings.

2.4.3 Analysis and discussion of computed features

In the following sections, the selected features are computed for all recordings in the available datasets and a high-level comparison between the results for the different datasets is presented. The results are presented as a boxplot, representing the distribution of the feature values for each dataset. Significant differences between on the one hand the TNO dataset (likely tampered vehicles), and on the other hand the KTM and KU Leuven datasets and the measurements from the validation campaign at TU Graz (all untampered vehicles), could suggest that a feature is a good candidate for detecting tampering. However, only indicative conclusions can be derived from this analysis as the differences in measurement and driving conditions between the different datasets are likely to have a large influence on the computed features. All features will be analysed in more detail during the processing of the larger and uniform datasets of the LENS in-field surveys.

This project has received funding from the European Union's Horizon Europe research and innovation programme under grant agreement No 101056777

2.4.3.1 Time domain features

Figure 5 presents the distribution of the skewness and kurtosis of the different datasets. All measurements show a negative skewness, indicating an asymmetric distribution with a longer tail towards negative values. The kurtosis of all datasets is as could be expected around 3. Although the observations should be interpreted with the necessary caution, the comparison of the different datasets seems to suggest that the TNO dataset containing vehicles suspected of being tampered has a slightly higher skewness and lower kurtosis.

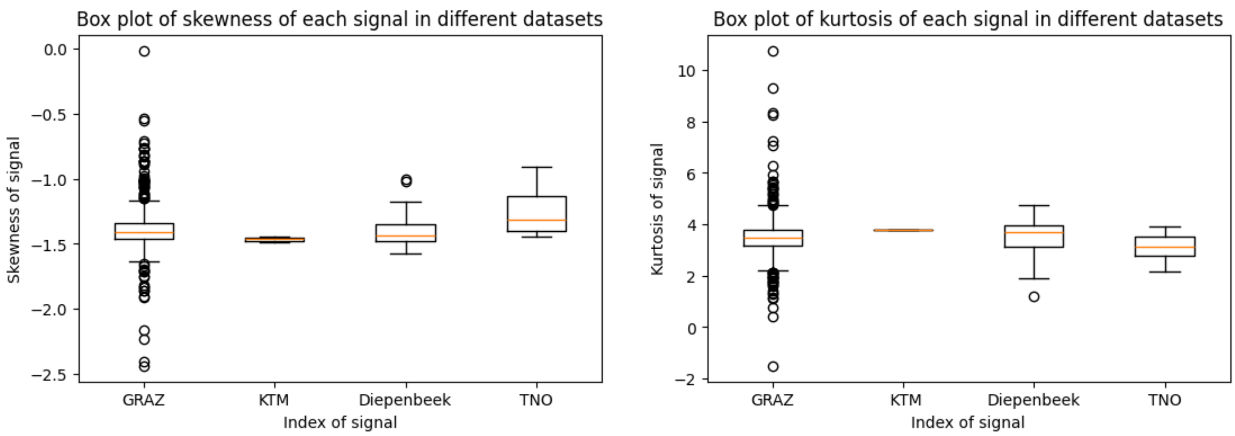

Figure 5: Distribution of the skewness and kurtosis, computed for each signal in the different datasets.

2.4.3.2 Frequency and time-frequency domain features

Many anomaly detection and sound classification techniques rely on a TFR of the measured signals, but often AI methods are required to extract the relevant information from such rich representation. Such approaches will be studied on the datasets gathered during the in-field surveys and detailed in D5.3, this section focuses on a preliminary analysis of some simple time-frequency domain features.

Figure 6 represents the centre of gravity of the one-third octave band spectrum of each signal in the datasets. The spectra of the signals in the TNO dataset on average have a higher centre of gravity, implying more high frequency content, than the other datasets. This is likely due to higher engine orders being more pronounced in the signals of the TNO dataset, a known characteristic of many tampered vehicles.

This project has received funding from the European Union's Horizon Europe research and innovation programme under grant agreement No 101056777

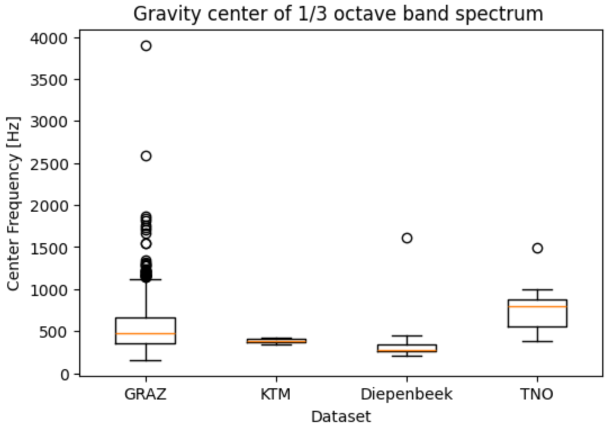

Figure 6: Distribution of the centre of gravity of the one-third octave band spectrum of the signals in each of the datasets.

A more direct metric for the prominence of the higher engine orders is the number of orders with a level above a certain threshold compared to the loudest order. The computation of this feature first requires the identification of the orders, using the technique described in section 2.3.1.3. Figure 7 shows the distribution of the number of orders within 12 dB of the loudest one for the different datasets. Also here, the TNO dataset clearly stands out and the difference with the other datasets is more pronounced than for the centre of gravity of the spectrum. This result illustrates the added value of features obtained with more advanced signal processing compared to simple metrics computed directly from the spectrum.

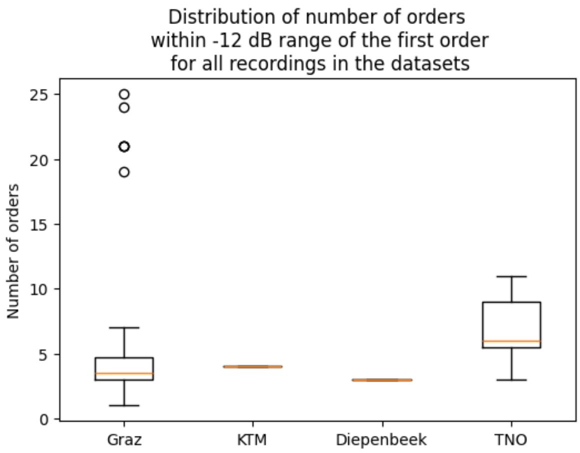

Figure 7: Distribution of number of orders within –12 dB of the first order for recordings in different datasets.

2.4.3.3 Psychoacoustic features

Psychoacoustic metrics quantify aspects of the human perception of sound. Since several types of tampering are known to, and sometimes done to affect the sound character, it is expected that these metrics also carry valuable information on the vehicle state.

Figure 8 shows the distribution of the maximum tone-to-noise ratio (TTNR) and prominence ratio (PR) for all recordings. A clear difference can be observed between the TNO dataset and the other datasets, which the former showing higher values for both metrics. This was expected as the TTNR and PR are mostly

This project has received funding from the European Union's Horizon Europe research and innovation programme under grant agreement No 101056777

characterizing the importance of the engine orders in the spectrum and it is known that these orders tend to be louder for tampered vehicles.

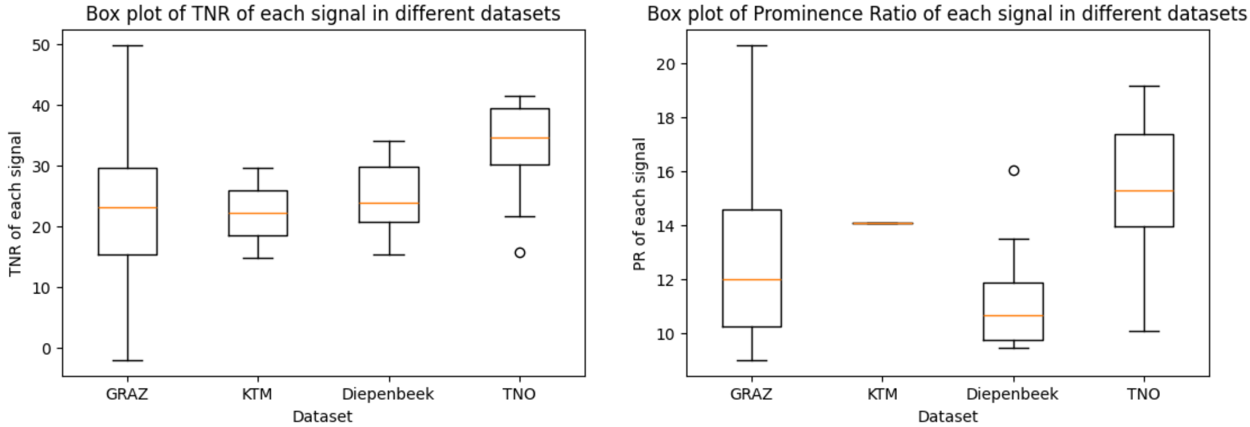

Figure 8: Distribution of the maximum tone-to-noise ration and prominence ratio for all recordings in the datasets.

Figure 9 shows the computed roughness for all recordings. Here the KTM dataset stands out compared to the others. For this dataset, a much larger roughness than the KU Leuven (Diepenbeek) dataset was expected. Both datasets consider a single vehicle, respectively a KTM Duke 125 and a BMW R1200 GS, of which the sound characters are very different by design. The other datasets contain multiple vehicles, hence the larger spread on the computed roughness. This result therefore does not necessarily indicate that roughness is not a suitable indicator for tampering, but highlights the fact that the noise character is very different for different L-vehicle categories. Some indicators, especially metrics quantifying aspects of the human perception of sound, should therefore better be analysed per vehicle category. Such analysis requires a sufficiently large dataset per vehicle category and could not yet be performed with the available data.

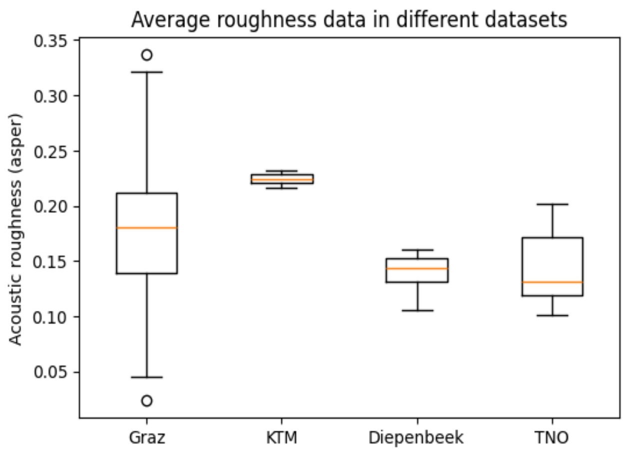

Figure 9: distribution of roughness for all recordings in the datasets.

This project has received funding from the European Union's Horizon Europe research and innovation programme under grant agreement No 101056777

2.4.3.4 Conclusion

In this section, a preliminary analysis of candidate features to identify tampered vehicles from noise measurements was conducted. Although the conclusions should be considered with care due to the differences between datasets, the results suggest that relevant features can be defined based on the time signals themselves, their time-frequency representation and psychoacoustic metrics. Although clear differences could already be observed with relatively simple features, it is expected that (the combination with) more complex features and/or AI methods will result in a more robust tampering detection.

This project has received funding from the European Union's Horizon Europe research and innovation programme under grant agreement No 101056777

3 Point sampling system

3.1 Previous work and literature review

In the LENS project we set-up on the point sampling approach from the H2020 project CARES (Grant Agreement No. 814966), where TU Graz developed and verified the general approach of roadside point sampling (PS) measurements. For the tampering detection of L-vehs in the LENS project, TUG examines the feasibility of the approach and will develop adaptations for the characteristics of L-vehs.

An intercomparison of PS to remote emission sensing with three PEMS-equipped test vehicles from category M1 (passenger cars) was done in the CARES project. The investigation validated the PS approach for particle and NOx measurements for both, high (EURO 4) and low (EURO 6b) emitters. The results were confirmed by analysis of data from several thousand vehicles from in-field measurements [16]. The coefficient of determination between PS and PEMS was found to be around $R^2 = 0.6$ for particle emissions. Results for NOx showed a relative deviation of 21 %.

No study of roadside emission measurements of L-vehs is known to the authors up to now.

3.2 Measurement setup

The general setup is shown in Figure 10. From a sampling position roadside, a gas sample is extracted and delivered to the analysers in the point sampling shelter. Three light barriers across the road, detect passing vehicles, assign a timestamp and allow the measurement of speed and acceleration. A radar sensor is used to differentiate between the vehicle types and for redundant vehicle detection, speed and acceleration measurement. Analysis of the vehicle length indicates if the passing vehicle is from category-L. The automated number plate recognition was realised by custom-made raspberry pi system with a raspberry pi camera. All devices, including the analysers, are connected to a common server for data collection, system control and a real-time cloud-uplink for selected data channels.

The gas sample is analysed for gaseous and particulate pollutants, for the device validation measurements and the first measurement campaign in Leuven (BE) we used a custom-made photoacoustic instrument for PM measurement, a commercial PN-counter based on diffusion charging, a TSI 3090 Engine Exhaust Particle Sizer (EEPS), and an Airyx iCAD gas analyser for CO_2 and NOx concentration measurement. It is intended to use the same set of instruments for the upcoming campaigns.

During the measurement campaigns, the gas analysers are recording continuously, and the data is assigned with a timestamp which is synchronised with internet time. Passing vehicles are detected by the light barriers to align the ANPR (Automatic Number Plate Recognition) data with the concentration data. All data is pre-processed and stored in a common database and uploaded in real time to a cloud, the processing is described below.

This project has received funding from the European Union's Horizon Europe research and innovation programme under grant agreement No 101056777

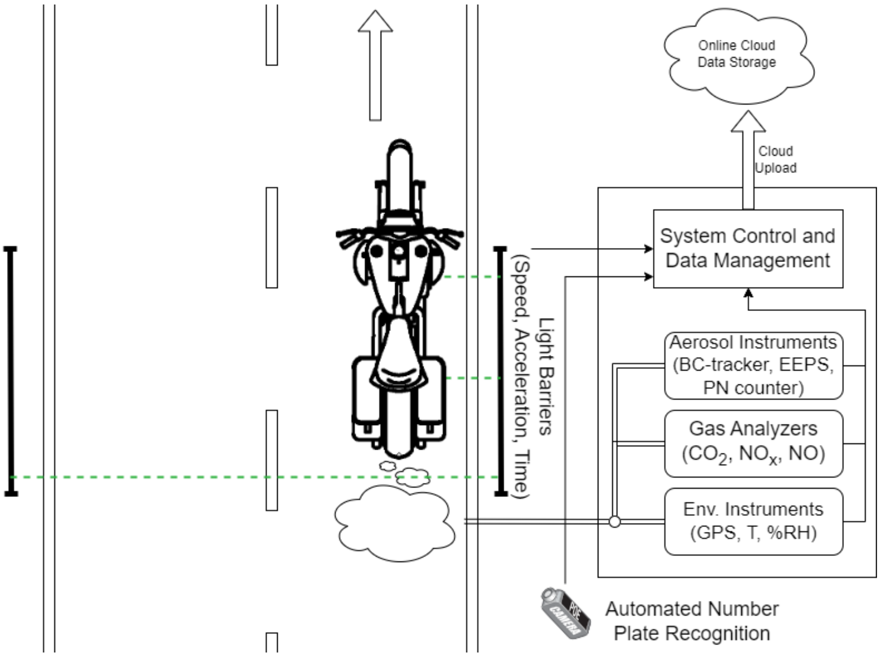

Figure 10: Scheme of the roadside point sampling setup for the in-field campaigns.

3.2.1 Signal processing and data management

Long-term roadside measurements create vast amount of data, what creates the need of an automated data management strategy and automated analysis. For the TU Graz PS system, we created the solution as indicated in Figure 11. The data from the subsystems (i.e. separate devices) is collected by a system control PC with internet connection, pre-processed and stored in a common SQL database. The pre-processing means alignment of the data format and sample rate, and assignment of a timestamp. Each sub-system itself already provides measured data, additional raw signal analysis is not necessary. The data from SQL database is uploaded to a secure cloud storage in real-time for live monitoring and analysis.

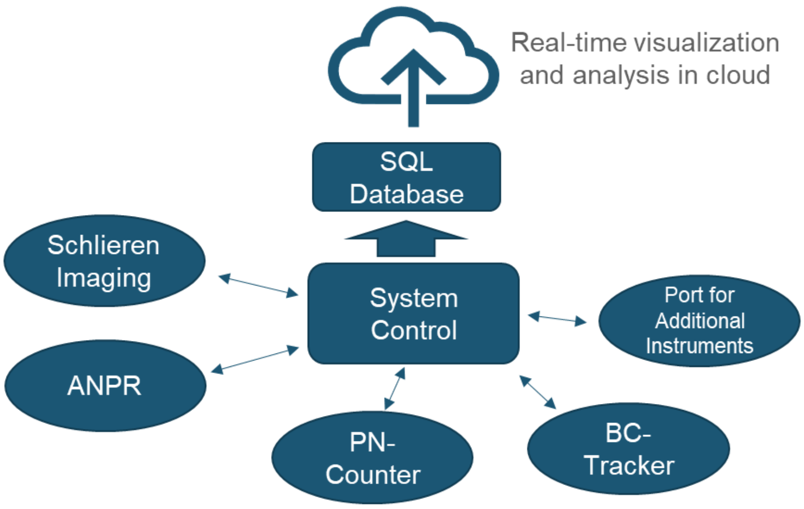

Figure 11: Scheme of the data management approach at the in-field measurement campaigns.

This project has received funding from the European Union's Horizon Europe research and innovation programme under grant agreement No 101056777

In the obtained data the concentration peaks might not be aligned correctly, due to device specific response times and the different sample flows. Thus, first an alignment of the peaks is necessary. From the aligned data, the relevant events must be identified, by comparison with the light barrier data. The according concentration peaks are then analysed for concentration correlation. The detailed approach is described in [17]. A scheme of the procedure is shown below in Figure 12.

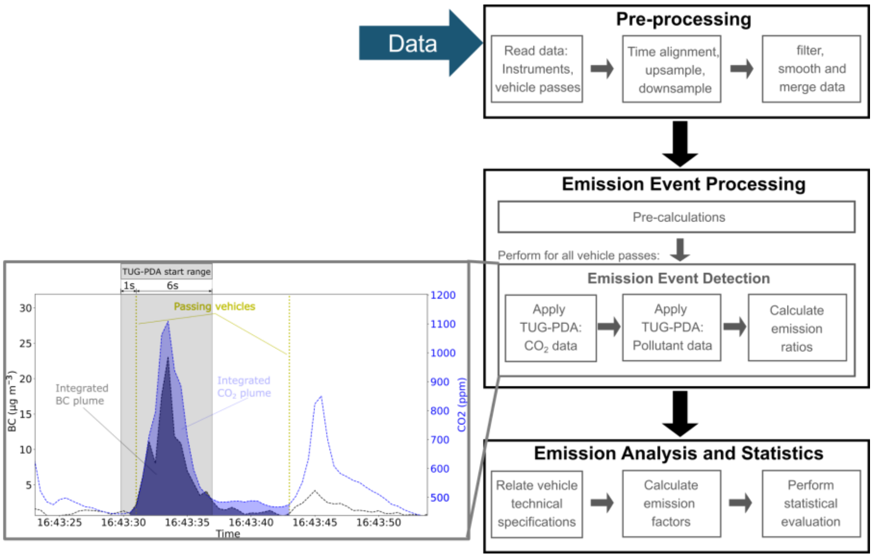

Figure 12: Scheme data analysis process and principle function of the peak detection algorithm.

The ANPR uses an AI-based algorithm for fast and reliable character recognition. The appropriate image is identified by the trigger from the light barriers. A Python programme is used to analyse the image for the number plate by pattern recognition and the respective area is cropped out. The image is then converted to binary and blurred to dilate the characters. From this, masks are created to crop out the characters which are then analysed by the Tesseract OCR. The algorithm must be adopted to the format and colours of number plates in the country of the measurement campaign and trained with images of number plates for reliable detection.

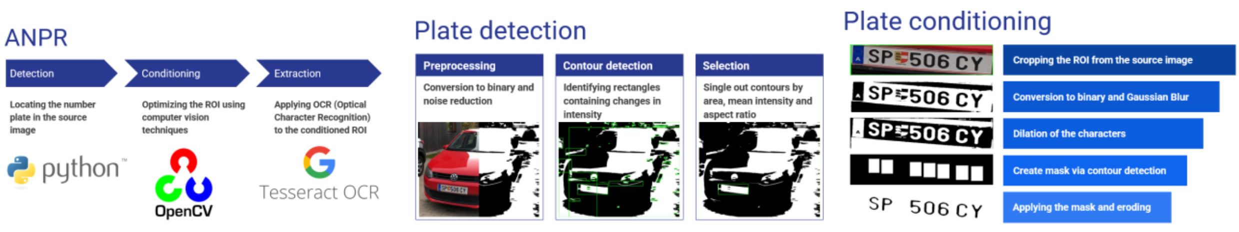

Figure 13: Schematic representation of the ANPR system image analysis.

3.3 Calibration and comparison of black carbon instruments

3.3.1 Goal of the efforts and description of the devices

The measurement of black carbon (BC) concentration is one important part in roadside PS, as currently this is the only possibility to measure particle emissions remotely. In the PS setup of TU Graz, a custom-made BC instrument, the “BC-tracker”, is used. For a reliable measurement in all upcoming PS efforts, we planned

This project has received funding from the European Union's Horizon Europe research and innovation programme under grant agreement No 101056777

for a calibration and a comprehensive device characterization in comparison to a commercial photoacoustic soot sensor, an AVL MSS2, and a commercial aethalometer, a MAGEE Scientific AE33. The aim was to determine the device behaviour for mass BC concentrations and different operation points, with different particle sizes and different organic content. The MSS2 was factory calibrated using gravimetric filter weighting and as used as the reference instrument.

The BC-tracker combines a custom-made photoacoustic cell for BC measurement and a commercial CO_2 sensor, thus CO_2-based emission factors can be determined by the instrument. A scheme of the BC-tracker is in the figure below.

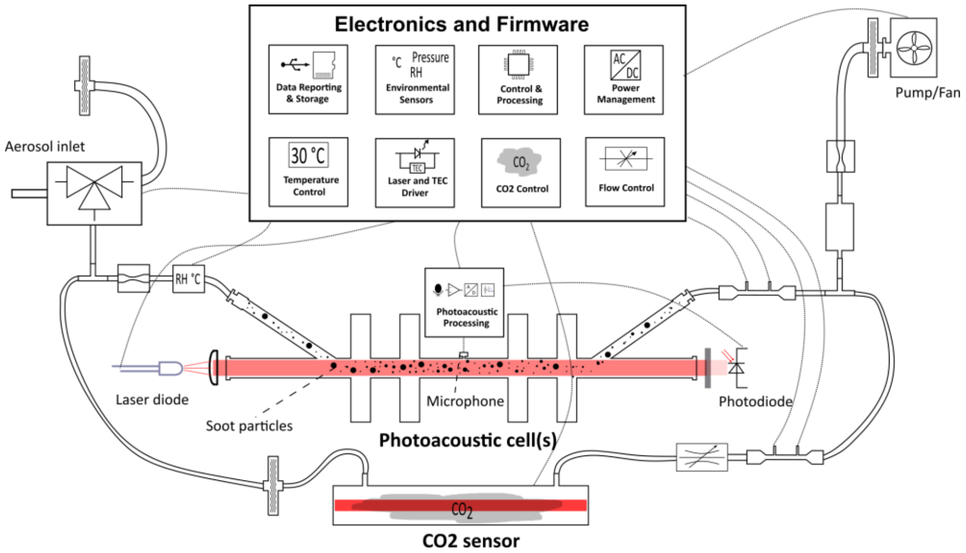

Figure 14: Scheme BC-tracker, as it was developed in CARES and is used in the LENS project.

With regard to a future compact PS instrument, we also included a quartz-enhanced photoacoustic (QEPAS) instrument, provided by the Lab of Applied Thermodynamics of Aristotle University via LENS partner Emisia.

The prototype photoacoustic, or optoacoustic, BC sensor has been developed through the EU Horizon Project RSENSE (Grant No. 862811) has also been mentioned at D3.1 and is used in LENS also as part of the EMISIA SEMS system for portable measurements. It has been compared to the other BC instruments described here to assess its applicability for roadside measurements. The Quartz Tuning Fork (QTF) that is used as a sound transducer offers both very high sensitivity (5µg/m3 at 1Hz sampling rate) and a fast dynamic response (<1s rising time). Complementary, the ellipsoid chamber protects the QTF from particle deposition and thus sensitivity loss, allowing for high concentration samples to be measured. The features described above make the prototype BC sensor a feasible candidate for roadside measurements of passing motorcycles. In Figure 15 you can see a schematic of the sensor`s operation principle.

This project has received funding from the European Union's Horizon Europe research and innovation programme under grant agreement No 101056777

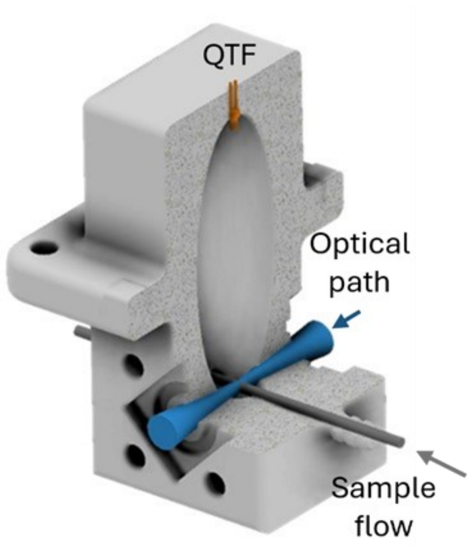

Figure 15: RSENSE BC Sensor schematic.

3.3.2 Setup and measurement plan

For the device calibration ad All instruments were used in parallel, using equally long tubes. Particles were generated either by a Jing miniCAST combustion soot generator or a PALAS DNP3000 spark soot generator. A catalytic stripper (CS) was used with the miniCAST to remove OC content from the soot. Subsequently the aerosol was guided through a dilution bridge to be able to vary the concentration. For measurements with monodisperse aerosol, we added a TSI DMA or a Cambustion AAC for size selection, followed by a dilution air inlet and a static mixer. The generated test aerosol was distributed to the instruments by a TSI four-way splitter made from stainless steel. For all operation points without the CS we loaded a quartz filter, to determine the actual EC/OC fraction by an offline analysis as a reference. We used a rotating disc diluter as the dilution bridge, as a the rotation speed scales directly with the dilution factor, namely a bisection of the rotation speed brought doubling of the dilution.

Three different tests were performed. First for measurement deviations for different particle sizes and EC/OC contents. For each operating point of the particle generator several concentrations were measured in intervals of two minutes. Starting at the highest concentration of the measurement series, each concentration step represents a doubling of the set dilution factor until noise level was reached, followed by a background measurement and an increase of the concentration in the same steps backwards. The second series was to test the linearity of the device responses at high concentrations. For these tests we increased the PM concentrations stepwise from ~ 100 µg/m³ to 1000 µg/m³. And third, we did dynamic tests by preselecting a certain concentration with the dilution bridge and then exposing the devices abruptly to the concentration for a defined amount of time, namely for 5, 10, 20 and 30 s.

This project has received funding from the European Union's Horizon Europe research and innovation programme under grant agreement No 101056777

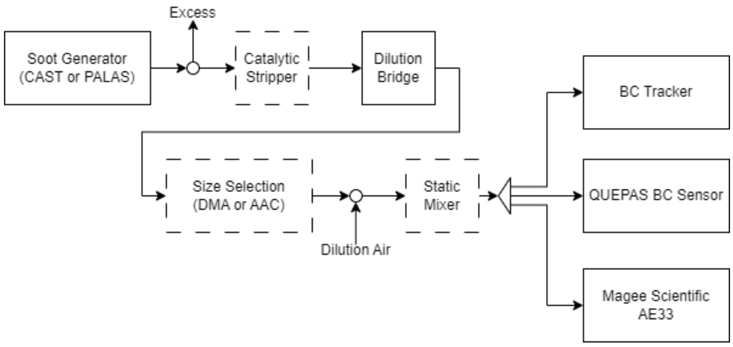

Figure 16: Flowchart of the characterization setup for the black carbon instrument calibration and comparison.

3.3.3 Results

For the linearity measurements for different EC/OC ratios and size distribution it can be seen in Figure 17, that the correlation between all instruments is very good for measurements with a Catalytic Stripper, thus for black carbon particles. Interestingly, only the AE33 shows deviations for the measurements with a particle GMD below 25 nm. For the data without CS, the linearity of is still very good for all devices, but the deviation in determined concentration is distinct. The proximity of the BC-tracker measurements to one of the AE33 channels is due to the fact, that the BC-tracker was calibrated using this AE33 channel.

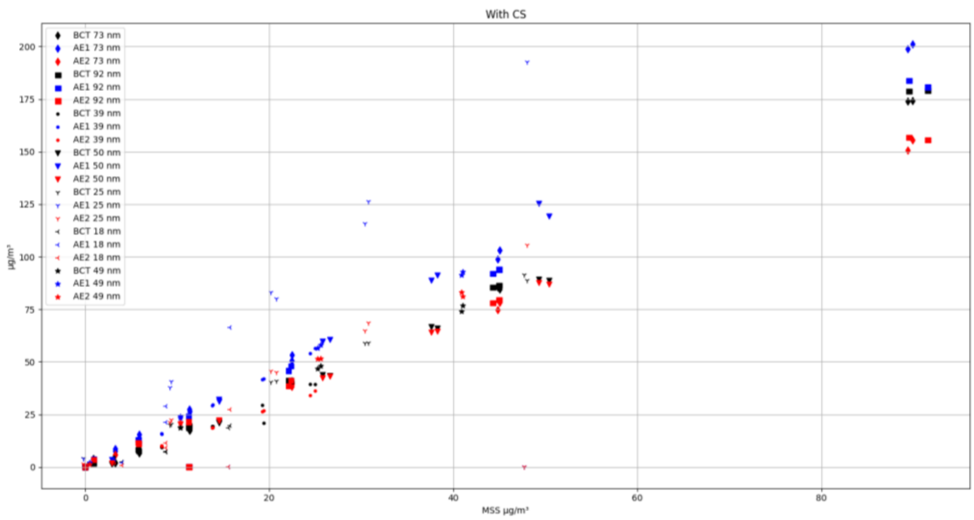

Figure 17: Correlation of the black carbon instruments to the reference device for different particle size distributions using a CS in the setup to generate EC particles.

This project has received funding from the European Union's Horizon Europe research and innovation programme under grant agreement No 101056777

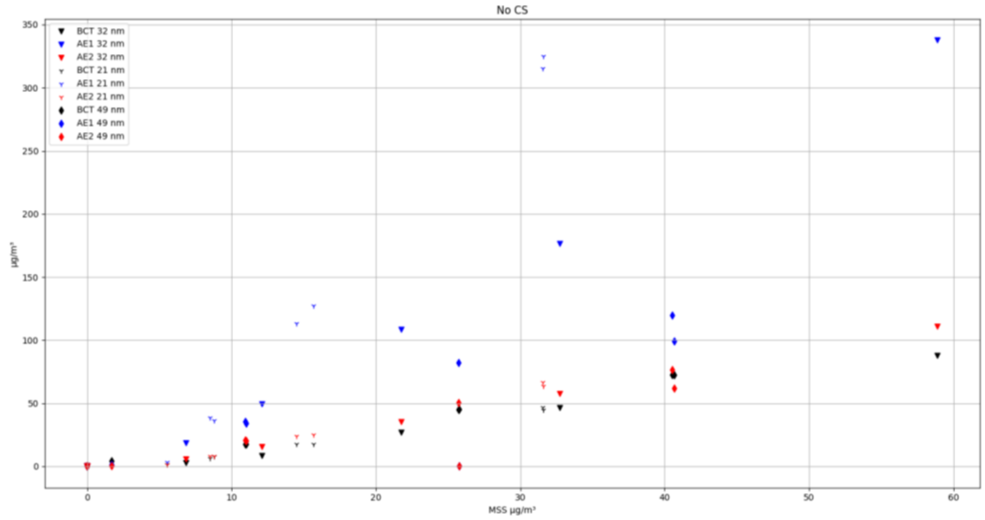

Figure 18: Correlation of the black carbon instruments to the reference device for different particle size distributions particles with OC content.

The linearity for high and very high particle mass concentrations can be seen in Figure 19. All devices show a linear behaviour until OP 5, while the measured difference in concentration is very high, the MSS shows around 600 µg/m³ while the AE33 and the BC-tracker show values above 1 mg/m³. Above these values the linearity of the AE33 is not given anymore, while the photoacoustic devices still how a linear behaviour. The decrease in concentration from OP5 to OP6 was due to a change in the setup, as the CS was removed to obtain higher concentrations.

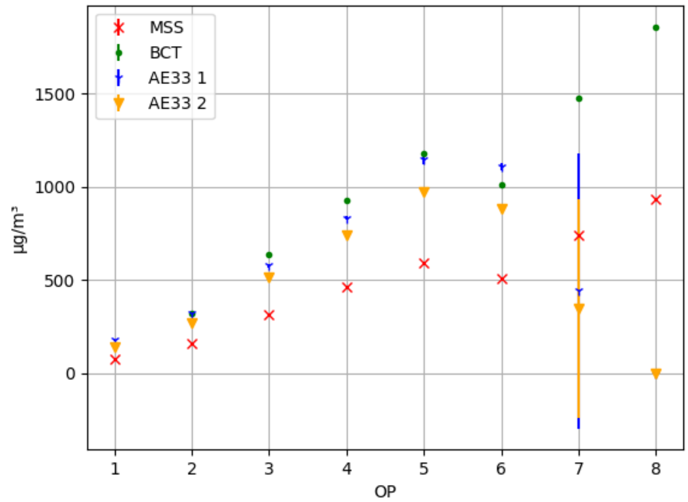

Figure 19: Results of the linearity measurements for high and very high soot mass concentrations.

The results from the dynamic tests are shown in Figure 20. For the 5 s exposure, the photoacoustic instruments reach the maximum concentrations, while the AE33 does not. The plateau can be identified for the first concentration for both, the BC-tracker and the MSS, while for the higher concentrations no steady state concentration is reached. A similar behaviour is observable for the 10 s exposure, where the BC-tracker and the MSS reach the plateau for all concentrations, while the AE33 response time is still not sufficient. For the 20 s and 30 s exposure all instruments reach the plateau concentration. Notable is the

This project has received funding from the European Union's Horizon Europe research and innovation programme under grant agreement No 101056777

difference in the absolute concentration measured. A difference between the AE33 and the photoacoustic instruments would be expectable, while the difference between the photoacoustic devices seems surprising. The latter can be explained by the different reference devices used for the calibration. While the MSS2 was calibrated using gravimetric filter weighting as a reference, the BC-tracker was calibrated using the AE33 channel 1 – what also explains the proximity of the signals.

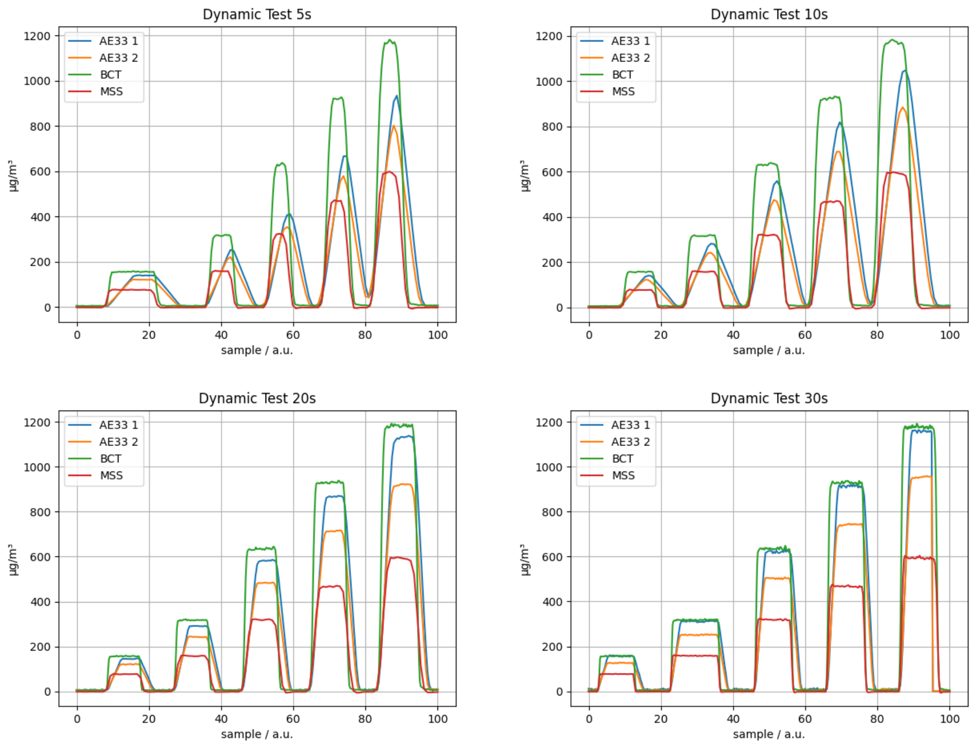

Figure 20: Results of the dynamic tests of the BC instruments for different exposure times.

This project has received funding from the European Union's Horizon Europe research and innovation programme under grant agreement No 101056777

4 Schlieren imaging system

4.1 Description of the measuring principle

A visualization of the exhaust plume would allow to follow the spread in the environment and could thus support the PS technique by an assessment of the capture by the PS sampling position. In the validation campaign the goal was to prove that the exhaust from L-vehs can be visualized by the technique at all in a basic, horizontal setup.

To visualize the spread of the exhaust plume, TU Graz participates with an experimental technique, based on Schlieren imaging. The Gas Schlieren Imaging Sensor (GSIS) system operates on Background Oriented Schlieren (BOS) imaging, is a well-known method for analysing fluid flows, which allows the visualization of variations in the refractive index. The principle is shown in Figure 21, exhaust causes a deflection (Ɛy) according to the refractive index of the gases present in the plume, resulting in a shift (Δy) in the image plane. If we compare an undistorted (reference) image to a distorted one, the difference between the reference image and the second image gives the Schlieren image and thus information about the object of interest.

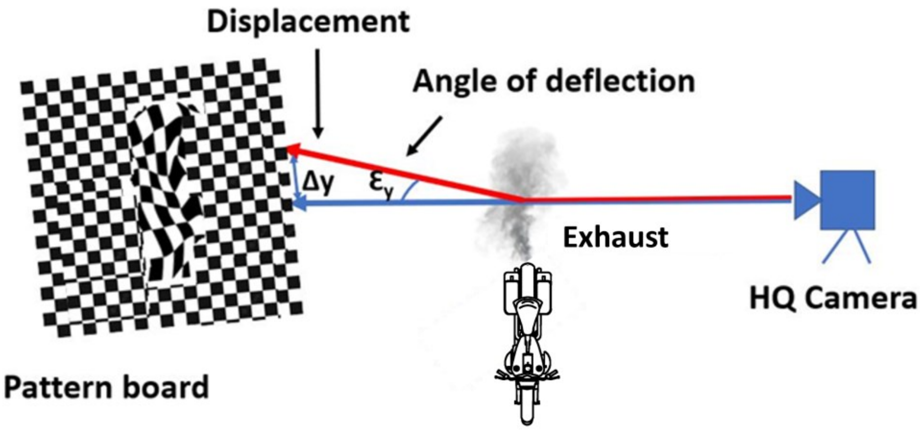

Figure 21: Schematic representation of the Schlieren Imaging setup.

4.2 Measurement setup

The GSIS system consists of a 12.3 MP HQ Raspberry Pi camera with a Sony IMX-477r camera chip, a Raspberry Pi 4B as a control unit to for the camera, a pattern board as a BOS background, a PC with an external GeForce RTX-3080 GPU for image processing and exhaust detection. The pattern board used was a random dot pattern with approximately 700,000 dots on a 1.5 m x 1.5 m plane, thus the camera resolution was about 3 times the number of dots on the pattern board.

The principal function of the GSIS system was verified in the scope of another project, a manuscript was submitted for publication.

This project has received funding from the European Union's Horizon Europe research and innovation programme under grant agreement No 101056777

4.3 Image processing

The detailed image processing for the GSIS system was developed in the scope of another project and was described in a manuscript was submitted for publication. Here follows a summary.

The images are converted to grayscale. Schlieren images are made by subtracting reference images from disturbed images; Each pixel in the distorted image is subtracted from the pixel in the reference image at the same position: After normalizing the image to increase contrast and focus on the most shifted pixels, blurring is applied to remove noise. Finally, thresholding assigns white to shifted pixels and black to the rest of the image. These images are called enhanced schlieren images. From these the YOLO v4 algorithm is used to detect the exhaust plume. The model uses a technique called spatial pyramid processing to extract features from the frames at different scales and resolutions. The model can detect objects of different sizes in one frame. The model is fast enough for real-time applications because it has only one stage and can be trained on a single GPU. We used about 700 enhanced Schlieren images of different exhaust plumes with a manually marked region of interest to train the model.

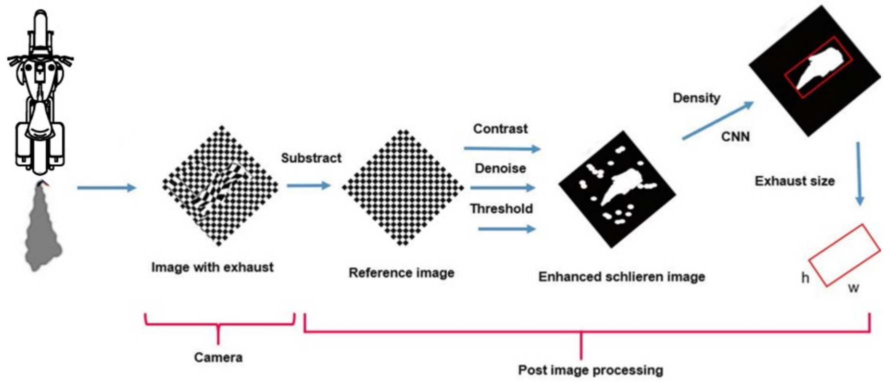

Figure 22: Schematic representation of the image processing steps to derive Schlieren Images and visualize exhaust.

This project has received funding from the European Union's Horizon Europe research and innovation programme under grant agreement No 101056777

5 Integrated system verification

5.1 Validation measurement campaign

5.1.1 Goal of the campaign

As the in-field measurement campaigns are linked with high-effort and are timely limited, the device operation and the feasibility of the chosen approaches was verified beforehand by a dedicated validation campaign carried out at the TU Graz campus. To establish a traceable relation between emission data acquired by roadside measurements with data from test bench (lab) and PEMS measurements, controlled vehicle passes of PEMS or SEMS equipped L-vehs have been done. The establishment of a relation between the PEMS and SEMS data to lab measurements is part of the efforts in WP3 and WP4. To validate the automatic order extraction from the noise measurements, the engine RPM measured by the vehicle's built-in sensor has been recorded during a few passes with a BMW C400X motorbike.

5.1.2 Validation of emission measurements by intercomparison of measurements

Measurements have been done at the 2-wheeler test bench at TU Graz with two motorbikes, a Husqvarna 701 Enduro with a 1 cylinder engine and 690 ccm displacement, and a KTM 390 Adventure, also 1 cylinder engine with 390 ccm displacement. The vehicles were equipped with a PEMS for the measurement of NOx, CO and CO_2. To establish a correlation between lab, PEMS and PS measurements, we installed the EEPS at the test bench with a sampling position at the dilution tunnel, parallel to the SPN 10 laboratory system. The emissions of the relevant gases were also measured from the tunnel by the test bench gas analyser.

For both motorcycles an RDC test was driven with the above-mentioned exhaust measurement devices measuring in parallel, the results are described in the next section.

5.1.3 Integrated system deployment and synchronisation

As shown in Figure 23, all roadside measurement systems for noise and pollutant emissions were deployed simultaneously at the campus Infeldgasse of TU Graz and measurements were conducted at various driving conditions using the following 5 motorbikes:

- Ride Omen 50,
- BMW C400X,
- KTM 125 Duke,
- KTM 790 Adventure,
- BMW XR1000.

The microphone array was mounted slightly lower (85 cm) during this campaign than during the in-field surveys for logistic reasons, but this should have no major impact on the results. During the measurement campaign, all measurement systems were thoroughly tested in realistic conditions, the acquisition settings of the individual measurement systems were finetuned and the possibility to synchronize the recordings of the different systems in postprocessing was verified. This is achieved based on the timestamps of the recordings and taking into account the relative positioning of the measurement systems, as well as the

This project has received funding from the European Union's Horizon Europe research and innovation programme under grant agreement No 101056777

driving direction and speed. The clocks of all measurement systems are synchronised via their internet connection.

Figure 23: Photography of the integrated measurement tests at the campus Inffeldgasse of TU Graz.

5.2 Results

5.2.1 Noise

The focus of the validation campaign for the noise measurement system was threefold:

1. Testing the triggering of the measurement system and finetuning the settings
2. Testing and validating the source localization method, described in section 2.3.1.1.
3. Testing and validating the order extraction technique, described in section 2.3.1.3.

Additionally, the noise measurements of this campaign are also a valuable dataset to evaluate different features. The results of this analysis have already been included in the comparison of the features for tampering detection in section 2.4.

5.2.1.1 Finetuning of the triggering settings

An important goal of the validation measurement campaign was to thoroughly test the automatic starting and stopping of the data logging when various types of L-vehicles drive past the microphone array. The measurement system has been programmed to continuously monitor the sound pressure measured by the first microphone of the array and to start a measurement when the measured sound pressure level exceeds

This project has received funding from the European Union's Horizon Europe research and innovation programme under grant agreement No 101056777

a threshold. This threshold needs to be set sufficiently high to avoid unwanted triggering of the system due to background noise events, but sufficiently low not to miss any L-vehicle drive by events. Similarly, a condition needs to be defined to stop the data logging. This needs to happen sufficiently after the vehicle passed the array to obtain signals of usable duration, but there also needs to be sufficient time before the next vehicle to store the buffered recording on the hard drive of the laptop and to rearm the measurement system before the next vehicle arrives.

Various settings have been tested throughout the measurement campaign and the most reliable approach, selected for the in-field surveys, is illustrated in Figure 24. The figure shows the typical evolution of the A-weighted sound pressure level LAF during the drive-by of an L-vehicle. The data logging starts when the sound pressure level exceeds a threshold. The value of this threshold is set on-site as it highly depends on the local situation (background noise, distance between the microphones and the driving lane, reflections on nearby buildings, etc.). Additionally, the background noise can change during the measurements and the threshold needs to be continuously reevaluated during the measurement campaign. The software has therefore been modified to enable adaptations of the trigger settings on the fly, without interrupting the measurements.

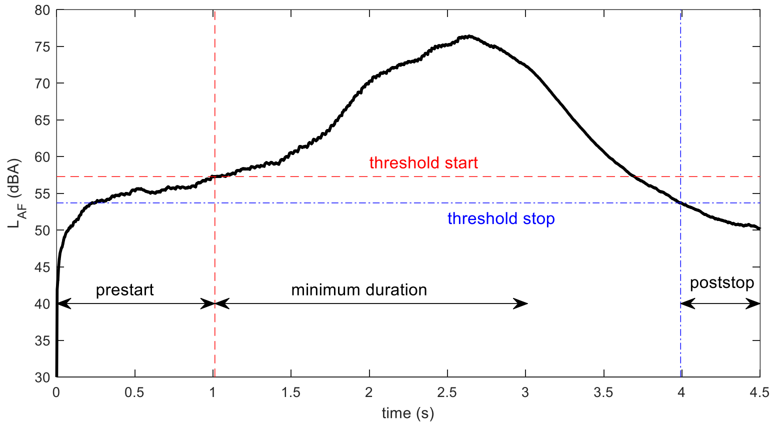

Figure 24: Illustration of the start and stop conditions for data logging.

During the measurement campaign, the system occasionally stopped the recording prematurely due to the fact that the sound pressure level is not a monotonically increasing function during the approach of the vehicle. Small oscillations of the instantaneous level during the approach of the vehicle can cause the data logging to start, but also to stop immediately. Hence, an approach has been developed to ensure that, after exceeding the threshold for starting a recording, the data logging doesn’t stop before the vehicle has passed. This is achieved by enforcing a minimum duration during which the stop condition is not monitored and the data logging doesn’t automatically stop. This minimum duration is usually set to 2s, but can be changed on-site, depending on the traffic intensity and spacing between vehicles. After the minimum duration, the data logging will be stopped when the sound pressure level at the first microphone position drops below a threshold. This threshold is usually set equal to the threshold for starting a recording, but can be adapted independently if needed.

As illustrated in Figure 24, the signal stored eventually to the hard drive extends 1s before the abovementioned start condition and 0,5s after the stop condition. These pre-start and post-stop durations have been implemented to avoid data loss due to the small latency in the system caused by the processing

This project has received funding from the European Union’s Horizon Europe research and innovation programme under grant agreement No 101056777

of the signals and the evaluation of the start and stop conditions. If needed, the pre-start and post-stop duration can be adapted.

5.2.1.2 Validation of the source localization technique

Knowing which recordings correspond to a vehicle passing past the microphone array on the driving lane of interest is crucial for the analysis of the in-field surveys as recordings of vehicles on other lanes will have a lower signal-to-noise ratio due to the larger distance between the vehicle and the array. This is the main goal of the source localization technique. During the measurement campaign, several runs pass the microphone array were carried out with a Ride Omen 50 scooter to validate the source localisation technique. This vehicle has a 1-cylinder 2-stroke engine and a CVT transmission. Although the EFR is lower, the highest peak in the spectrum in the range between 200 Hz and 400 Hz has been used to generate the beamforming maps. This frequency range is the result of a compromise. Lower frequencies, such as the EFR, would result in a poor spatial resolution. At higher frequencies, the contribution of the L-vehicle to the noise spectrum will be lower and background noise sources will have a larger influence on the result.

Figure 25 shows the beamforming map for two passes, one uphill (going from -90° to +90°) and one downhill (driving from +90° to -90°), of the Ride Omen 50 scooter. In both cases, the trajectory corresponding to the vehicle can clearly be identified as the diagonal line of high intensity in the map. Since no roads with multiple lanes per driving direction will be considered during the in-field surveys, these results show that the noise recording itself is sufficient to identify the lane on which the vehicle was driving as long as the noise recording is dominated by a single vehicle.

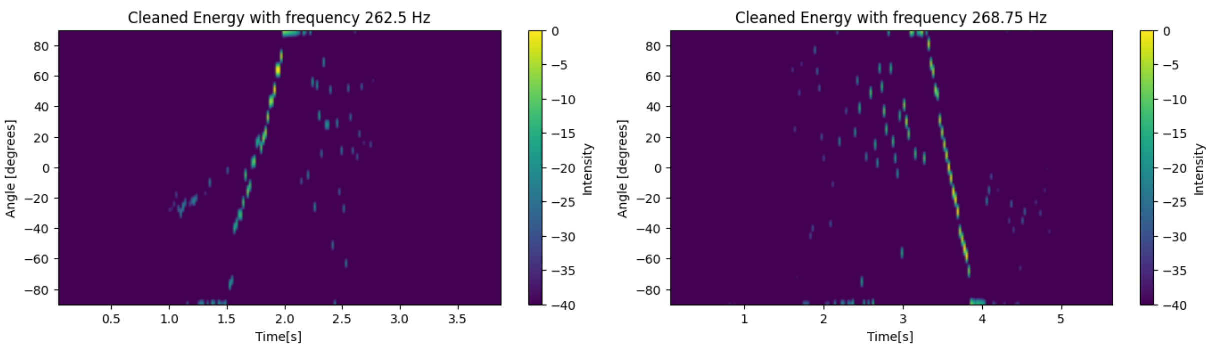

Figure 25: Beamforming map of an uphill (left) and downhill (right) pass of the Ride Omen 50 scooter with the engine running at full speed.

Figure 26 shows the beamforming map of a more challenging situation, where two L-vehicles are driving very close one after the other: a Ride Omen 50 scooter passing the array around 2.5s after the start of the recording and a BMW XR1000 passing the array around 3.5s. The second vehicle is clearly the loudest and its trace is clearly visible in the beamforming map. However, many other artefacts are visible in the map and the trace of the first vehicle is difficult to recognize. This is due to the fact that the noise contributions of both vehicles interfere with each other during the entire recording. Although it may still be possible to extract the contribution of the loudest vehicle by focusing on its trace in the map for this particular case with one clearly dominant noise contributor, this is not always the case and more advanced techniques would be needed to separate source contributions in a more general case. The need for such techniques will be evaluated based on the recordings collected during the in-field surveys.

This project has received funding from the European Union's Horizon Europe research and innovation programme under grant agreement No 101056777

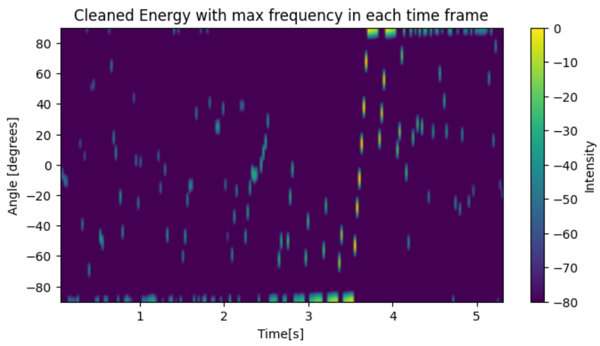

Figure 26: Beamforming map of an uphill pass of the Ride Omen 50 scooter directly followed by a louder BMW XR1000 motorcycle.

5.2.1.3 Validation of the order extraction method

During a part of the measurement campaign, a BMW C400X was equipped with a logging system to store the engine speed measured by the vehicle's onboard sensors. After synchronisation, this data can be compared with the engine rpm estimated from the orders, extracted from the noise measurements.

Figure 27 shows the engine rpm measured by the BMW C400x's onboard sensors during a series of runs past the microphone array, numbered from 1 to 9. Every time the motorcycle passes in front of the microphone array, a noise recording is started. The first peak in the rpm is a downhill positioning run during which the vehicle did not pass the array and no noise recording was started. The focus of the measurement session is on the uphill runs, labelled with an odd number, during which the motorcycle drives close to the microphone array mimicking the measurement conditions of the in-field surveys. The downhill runs (even number) for repositioning the vehicle are nevertheless also recorded. For each recording, the spectrogram of the signals is calculated and the orders are extracted as described in section 2.3.1.3. For this vehicle with a 1-cylinder 4-stroke engine, the EFR is the 1/2th order and the rpm is therefore estimated by scaling the extracted fundamental frequency with a factor 120. This result is added to the graph for comparison. A good agreement can be observed, but some discrepancies can be observed towards the end of the individual noise recordings. This is due to the lower signal-to-noise ratio when the vehicle is further from the microphone array.

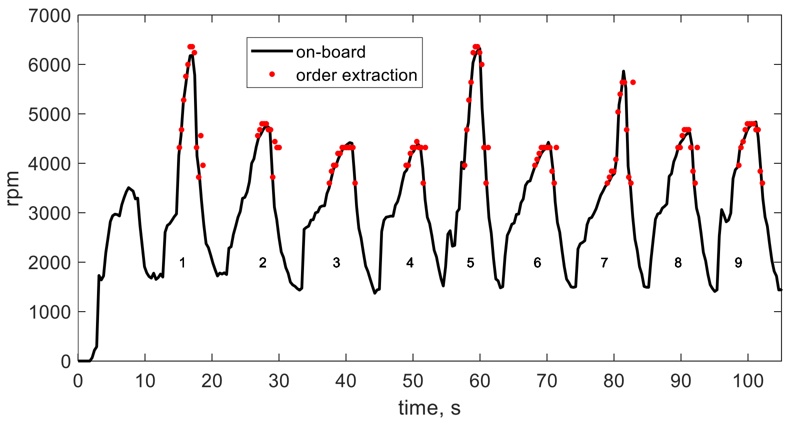

Figure 27: Engine rpm of the BMW C400X during a series of runs past the microphone array, measured using the onboard sensor and estimated from the roadside noise measurements.

This project has received funding from the European Union's Horizon Europe research and innovation programme under grant agreement No 101056777

The effect of the distance and signal-to-noise ratio is illustrated in Figure 28, showing the spectrogram and the corresponding overall sound pressure level for the 7th run past the microphone array. The EFR, measured with the onboard sensor and estimated from the noise measurements, and its harmonics are also indicated on the spectrogram. The overall sound pressure level is clearly highest when the vehicle passes closest to the microphone. At the beginning and end of the recording, the vehicle is further away and the sound pressure level is almost 20dB lower. The signal-to-noise ratio is then significantly lower and the engine orders less prominent, and hence more difficult to identify. In this particular case, the strong tones present in the background noise at multiples of 52 Hz are the dominant tonal content of the spectrum and lead to a wrong estimation of the engine rpm at the end of the recording. However, considering the part of the recording where the contribution of the L-vehicle noise dominates the measured sound pressure, a good agreement between the measured and estimated engine rpm is obtained. Hence, the orders extracted from this part of the recordings can be used for computing features characterizing the passing vehicle's state as discussed in section 2.4.2.

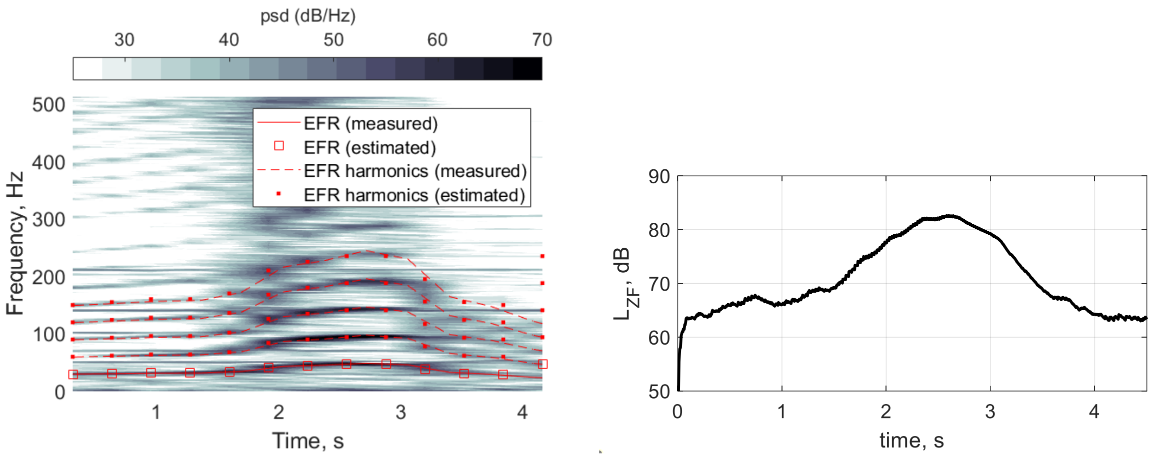

Figure 28: (left) spectrogram of run 7 past the microphone array with the BMW C400X and the EFR and its harmonics measured by the onboard sensor and estimated from the extracted orders. (right) corresponding evolution of the sound pressure level.

5.2.2 Intercomparison of emission measurements

Comparison of the instruments at the test bench

The agreement of the measurement results from the test bench are very good, as it can be seen in Figure 29. The coefficient of determination for PN between the EEPS to the SPN10 measurement system was determined to R^2 = 0,95 and for NOx, between the test bench analyser and the PEMS to R^2 = 0,99.

This project has received funding from the European Union's Horizon Europe research and innovation programme under grant agreement No 101056777

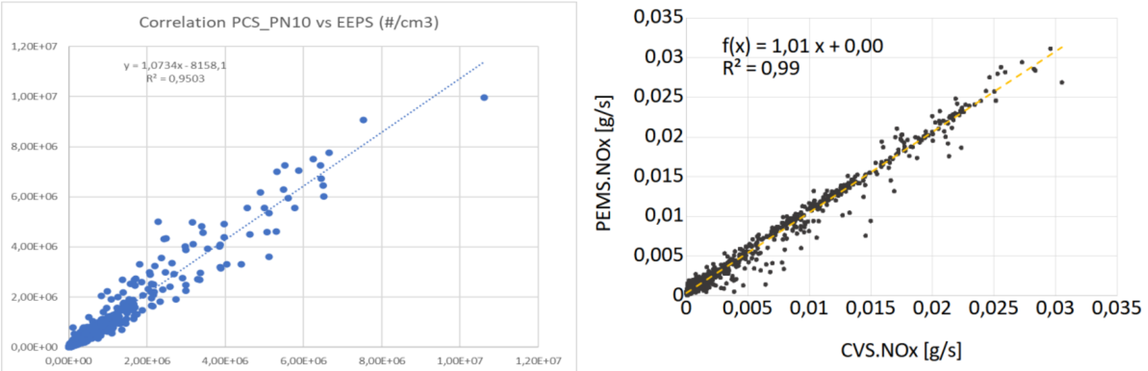

Figure 29: Correlation plots of the EEPS to the test bench PN measurement (left) and of the PEMS to the NOx measurement in the dilution tunnel (right).

Comparison of PS and PEMS

The correlation of the data from the validation campaign between PEMS and the PS measurement is poor. The best results have been apparently obtained for NO_2, with R^2 = 0,69. The spread of the datapoints relativises this value and from the exemplary time series data it is evident that the pass by was hardly detected at all. From the obtained data it was very difficult to determine a reliable measured value at these signal levels. Please note that the correlation of the instrument at the test bench was very good. The identification of the time delay between PEMS and the PS signal was possible by UTC timestamps and the prior evaluation of the sample and response time of the instruments in the PS setup.

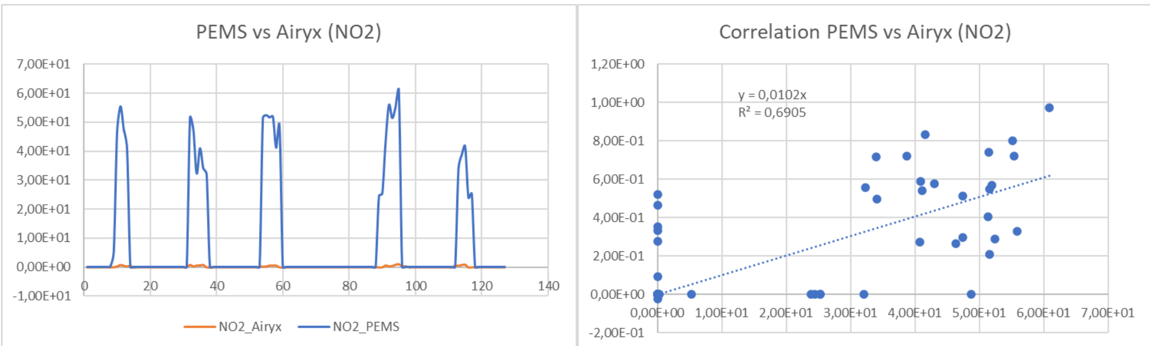

Figure 30: Results for the comparison of the NOx measurements from PS and PEMS. Time series (left) and correlation plot (right).

For the particle measurements the obtained correlation between PEMS and PS with the EEPS was quantified by R^2 = 0,23. The exemplary time series is comparable to the NO_2-data, the analysis revealed that even a detection of the pass by of the LVs was hardly possible. The determination of a measured value was only possible for a small number of cases, as shown in Figure 31 right.

This project has received funding from the European Union's Horizon Europe research and innovation programme under grant agreement No 101056777

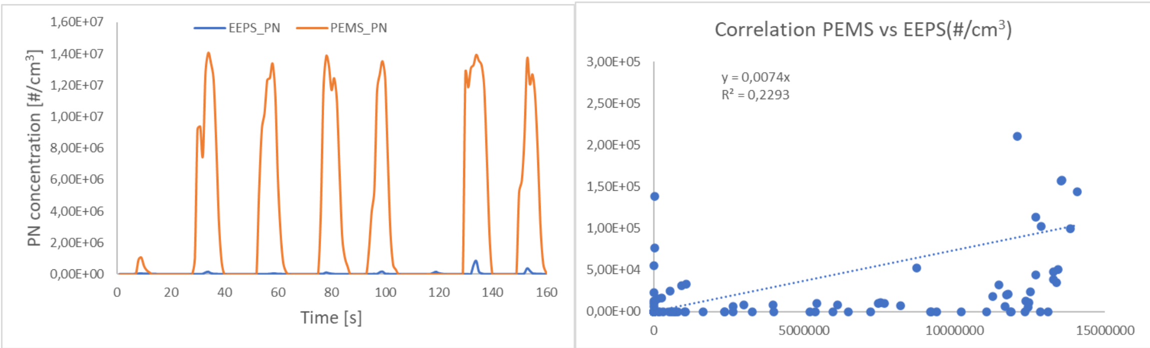

Figure 31: Results for the comparison of the particle number measurements from PS and PEMS. Time series (left) and correlation plot (right).

The PS measurements of CO_2 with the BC-tracker have been almost impossible, as the detected concentrations have been around ambient levels. In Figure 32 left, the data seems to be promising, but the signal was set to 0 in post processing for all times which are not linked to a vehicle pass. The detection of a passing L-veh was not possible from the CO_2 data. From the datapoints in the correlation plot it is apparent, that a correlation actually not given. The obtained $R^2 = 0{,}61$ can be considered as a statistical artifact.

The measurement of a BC concentration was not possible at all in the validation campaign, although the pre-evaluation of the data from the 1st in-field campaign in Leuven shows some valid BC measurements. Details on this will be included in the next WP5 report.

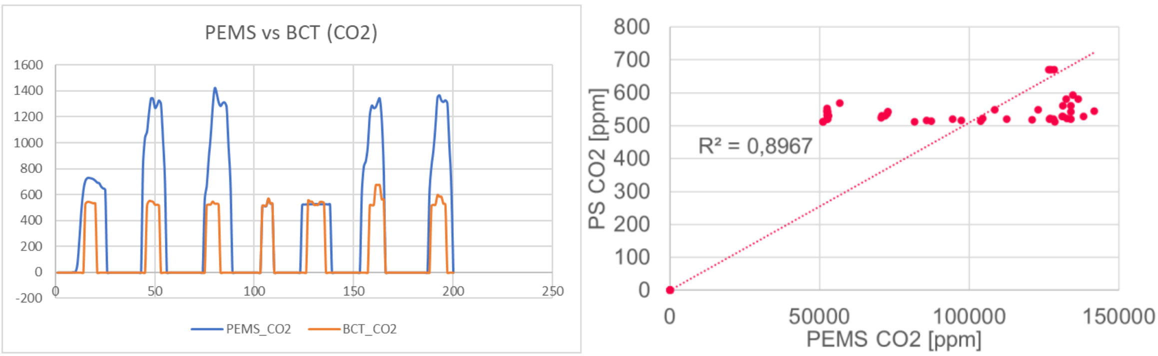

Figure 32: Results for the comparison of the CO_2 measurements from PS and PEMS. Time series (left) and correlation plot (right). The CO_2 concentration was set 0 in post processing for all data which was not linked to a vehicle pass.

The difficulty of PS measurements for L-vehs is probably due to the low exhaust mass flows. Although the concentrations of pollutants are very high compared to passenger cars and heavy-duty vehicles with exhaust aftertreatment systems, the absolute amount of pollutant per vehicle is comparably low. A concentration measurement from a diluted plume is thus hardly possible. The calculation of emission factors from the PS-data was omitted due to the unreliable data. The lack of correlation between PEMS and PS should not be interpreted as a bottleneck for the continuation of the study, as the motorcycle(s) used in this campaign were overall of low emission levels. As the PS will primarily be used for the identification of ultra-emitters, we expect this to be able to detect these high concentration levels produced by such vehicles.

This project has received funding from the European Union's Horizon Europe research and innovation programme under grant agreement No 101056777

5.2.3 Schlieren

The experiments with the schlieren imaging setup to visualize the exhaust from L-vehs gave promising results, as the exhaust can be visualised throughout for all vehicle passes, as shown in the exemplary images below for the Ride Omen 50 and the KTM Duke 125. The validation can be considered as successful as the exhaust can be visualized by the technique. For the in-field campaign a setup will be chosen to follow the spread of the exhaust from the vehicle and assess the capture by the position of the PS sampling spot.

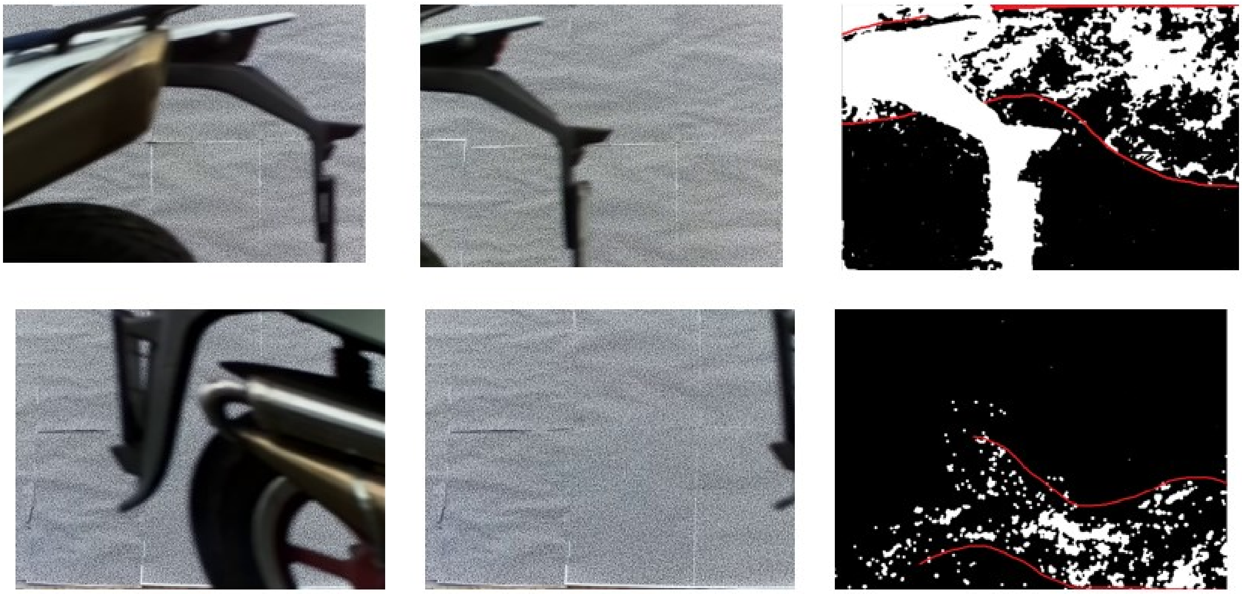

Figure 33: Exemplary images to illustrate the exhaust gas visualization of passing L-vehs.

This project has received funding from the European Union's Horizon Europe research and innovation programme under grant agreement No 101056777

6 Conclusion

This deliverable described the development of methods for detecting tampered / high-emitting L-category vehicles using roadside measurements of noise and pollutant emissions. The approaches based on noise and pollutants have first been developed as independent systems and their measurement results are synchronized in postprocessing.

The noise measurement system consists of a microphone array, a data acquisition system and a laptop for data storage and processing. The signal processing toolchain is modular and computes a number of features, which carry information about the state of the vehicle. A preliminary analysis of promising features has been carried out based on available noise datasets. These features will eventually be further processed by the detection algorithm. The training of this algorithm will be done using the labelled noise measurements for both tampered and untampered L-category vehicles from the LENS in-field surveys.

From the efforts until now we have to draw the main conclusion for roadside emission measurements, that the PS technique is very likely not feasible to detect tampered L-vehs reliably. The correlation between PS measurements of L-vehs equipped with PEMS was very poor and analysis the time series shows, that by PS a pass by can hardly be detected. This is very likely due to the comparably low exhaust mass flow from small engines. Although the pollutant concentration in the exhaust is high (according to data from WPs 3 and 4), the total emitted amount is very low, so that single passing vehicles do not cause concentration events which are detectable roadside. But the implied conclusion and the hypothesis are still the subject of research in LENS. A reliable final statement will be possible after analysing the results of the measurement campaigns in Paris and Barcelona and after repeating the correlation measurements with PEMS and PS.

The devices used for point sampling have been referenced either in the lab or at the test-bench at TU-Graz. The calibration campaign of the black carbon measurement instruments has shown that the behaviour of the used BC-tracker is reliable over a wide concentration range and unessentially influenced by the soot composition, in comparison to an aethalometer. The used reference device was calibrated by gravimetric filter weighting beforehand. The test bench measurements compared the PEMS measurements with the lab analysers of the test bench and an EEPS, which is also used for the PS efforts. The results show a very good correlation for all measurements.

The experiments with optical gas imaging by Schlieren Imaging have been successful to verify the principle of operation. The goal is to develop a setup which allows to visualize the spread of the plume and apply it at one in-field measurement campaign.

A validation measurement campaign, where all systems have been deployed together for the first time, has been carried out to thoroughly test and refine the noise and pollutant emission measurement approaches, their interoperability and their synchronization prior to the LENS in-field surveys. The results of these surveys will be reported in D5.3 of the LENS project.

This project has received funding from the European Union's Horizon Europe research and innovation programme under grant agreement No 101056777

7 References

[1] Batsalia N et al. (2023). LENS D5.1 L-vehicle tampering and undesirable effects. https://www.lens-horizoneurope.eu/wp-content/uploads/2024/07/D5.1.pdf

[2] Nave L and Mietlicki F (2019). Medusa, a new approach for noise management and control in urban environment. Proceedings of Internoise 2019.

[3] Mietlicki C, Mietlicki F and Bernfeld D (2022). Hydra: a noise radar to automatically track down excessively noisy vehicles in real traffic conditions. Proceedings of Internoise 2022.

[4] Automatically control noisy vehicles in your city. Online: https://dbflash-camera.com/en/accueil-en/. Last accessed on 26 July 2024.

[5] Agha A, Ranjan R and Gan W-S (2017). Noisy vehicle surveillance camera: A system to deter noisy vehicle in smart city. Applied Acoustics 117: 236-245. DOI: 10.1016/j.apacoust.2016.05.025

[6] NEMO, Monitoring Noise by Remote Sensing. online: https://nemo-cities.eu/remote-sensing-device-for-noise/. Last accessed on 26 July 2024.

[7] Dittrich M.G. (2024). Haalbaarheid van de geluidsflitspaal in Nederland. TNO report 2024 R10444. https://publications.tno.nl/publication/34642766/7vId7Dyt/TNO-2024-R10444.pdf

[8] National Traffic Safety and Environment Laboratory (2021). Development of automatic illegal replacement muffler detection system at NTSEL. 04th Session of the GRBP Task Force-Vehicle Sound (TF-VS), TFVS-04-08.

[9] National Traffic Safety and Environment Laboratory (2023). Illegal muffler vehicle detection system under development at NTSEL: Update of TFVS-14-04. 14th Session of the GRBP Task Force-Vehicle Sound (TF-VS).

[10] Cheng K W et al. (2023). Spectrogram-based classification on vehicles with modified loud exhausts via convolutional neural networks. Applied Acoustics 205: 109254. DOI: 10.1016/j.apacoust.2023.109254

[11] AKUT, Acoustic incident detection in tunnels. online: https://www.joanneum.at/digital/en/products/akut/. Last accessed on 17 July 2024.

[12] Amini A et al. (2016). Wayside detection of faults in railway axle bearings using time spectral kurtosis analysis on high-frequency acoustic emission signals. Advances in Mechanical Engineering 8(11): 1-9. DOI: 10.1177/1687814016676000

[13] Zhang D et al. (2020). Wayside acoustic detection of train bearings based on an enhanced spline-kernelled chirplet transform. Journal of Sound and Vibration 480:115401. DOI: 10.1016/j.jsv.2020.115401

[14] George J et al. (2013). Exploring Sound Signature for vehicle Detection and Classification Using ANN. International Journal on Soft Computing 4(2): 29-36. DOI: 10.5121/ijsc.2013.4203

[15] Zaman K, Sah M, Direkoglu C and Unoki M (2023). A Survey of Audio Classification Using Deep Learning. IEEE Access 11: 106620-106649. DOI: 10.1109/ACCESS.2023.3318015

[16] Siemens, Simcenter Scadas XS Hardware. Online: https://plm.sw.siemens.com/en-US/simcenter/physical-testing/scadas/xs/. Last accessed on 26 July 2024.

[17] PCB, ICP electret array microphone: model 130A24. Online: https://www.pcb.com/products?m=130a24. Last accessed on 26 July 2024.

[18] Sijtsma P (2007). CLEAN Based on Spatial Source Coherence. International Journal of Aeroacoustics 6(4):357-374. DOI: 10.1260/147547207783359459

This project has received funding from the European Union's Horizon Europe research and innovation programme under grant agreement No 101056777

[19] Randall RB (2017). A history of cepstrum analysis and its application to mechanical problems. Mechanical Systems and Signal Processing 97: 3-19. DOI: 10.1016/j.ymssp.2016.12.026

[20] Abdul Z K and Al-Talabani A K (2022). Mel Frequency Cepstral Coefficient and its Applications: A Review. IEEE Access 10: 122136-122158. DOI: 10.1109/ACCESS.2022.3223444

[21] Antoni J (2006). The Spectral Kurtosis: A Useful Tool for Characterising Non-Stationary Signals. Mechanical Systems and Signal Processing 20(2): 282–307.

[22] Antoni J and Randall RB (2006). The Spectral Kurtosis: Application to the Vibratory Surveillance and Diagnostics of Rotating Machines. Mechanical Systems and Signal Processing 20(2): 308–331.

[23] ECMA International (2022). ECMA-418: Psychoacoustic metrics for ITT equipment. Part 1: Prominent discrete tones.

[24] Gryllias K C and Antoniadis I A (2012). A Support Vector Machine approach based on physical model training for rolling element bearing fault detection in industrial environments. Engineering Applications of Artificial Intelligence 25(2):326-344. DOI: 10.1016/j.engappai.2011.09.010

[25] Verstraete D B et al. (2020). Deep semi-supervised generative adversarial fault diagnostics of rolling element bearings. Structural Health Monitoring 19(2:390–411. DOI: 10.1177/1475921719850576

[26] Dittrich M.G., Wessels P and Staats F (2022). Monitoring luide voertuigen in Amsterdam (Monitoring of loud vehicles in Amsterdam, in Dutch), TNO report ref. TNO 2022 R10053. https://openresearch.amsterdam/en/page/84173/rapport-tno-monitoring-luide-voertuigen-in-amsterdam

[27] Knoll, M., Penz, M., Schmidt, C., Pöhler, D., Rossi, T., Casadei, S., Bernard, Y., Hallquist, Ǻsa M., Sjödin, Ǻke, & Bergmann, A. (2024). Evaluation of the point sampling method and inter-comparison of remote emission sensing systems for screening real-world car emissions. Science of the Total Environment, 932(x). https://doi.org/10.1016/j.scitotenv.2024.171710

[28] Knoll, M., Penz, M., Juchem, H., Schmidt, C., Pöhler, D., & Bergmann, A. (2024). Large-scale automated emission measurement of individual vehicles with point sampling. Atmospheric Measurement Techniques, 17(8), 2481–2505. https://doi.org/10.5194/amt-17-2481-2024

This project has received funding from the European Union's Horizon Europe research and innovation programme under grant agreement No 101056777